

## Can Neutron-Star Mergers Explain the $r$ -process Enrichment in Globular Clusters?

MICHAEL ZEVIN,<sup>1,2,\*</sup> KYLE KREMER,<sup>1,2</sup> DANIEL M. SIEGEL,<sup>3,4</sup> SCOTT COUGHLIN,<sup>2</sup> BENNY T.-H. TSANG,<sup>5</sup>  
CHRISTOPHER P. L. BERRY,<sup>2</sup> AND VICKY KALOGERA<sup>1,2,6</sup>

<sup>1</sup>*Department of Physics and Astronomy, Northwestern University, 2145 Sheridan Road, Evanston, IL 60208, USA*

<sup>2</sup>*Center for Interdisciplinary Exploration and Research in Astrophysics (CIERA), 2145 Sheridan Road, Evanston, IL 60208, USA*

<sup>3</sup>*Perimeter Institute for Theoretical Physics, Waterloo, Ontario, Canada, N2L 2Y5*

<sup>4</sup>*Department of Physics, University of Guelph, Guelph, Ontario, Canada, N1G 2W1*

<sup>5</sup>*Kavli Institute for Theoretical Physics, University of California, Santa Barbara, CA 93106, USA*

<sup>6</sup>*CIFAR Fellow*

### ABSTRACT

Star-to-star dispersion of  $r$ -process elements has been observed in a significant number of old, metal-poor globular clusters. We investigate early-time neutron-star mergers as the mechanism for this enrichment. Through both numerical modeling and analytical arguments, we show that neutron-star mergers cannot be induced through dynamical interactions early in the history of the cluster, even when the most liberal assumptions about neutron-star segregation are assumed. Therefore, if neutron-star mergers are the primary mechanism for  $r$ -process dispersion in globular clusters, they likely result from the evolution of isolated, primordial binaries in the clusters. Through population modeling of double neutron-star progenitors, we find that most enrichment candidates are fast-merging systems that undergo a phase of mass transfer involving a naked He-star donor. Only models where a significant number of double neutron stars proceed through this phase give rise to enrichment fractions that are comparable to the observed number of enriched globular clusters. Under various assumptions for the initial properties of globular clusters, we find if the secondary phase of mass transfer from a naked He-star donor proceeds stably (unstably), a neutron-star merger with the potential for enrichment will occur in  $\sim 2-12\%$  ( $\sim 4-25\%$ ) of globular clusters. The strong anti-correlation between the pre-supernova orbital separation and post-supernova systemic velocity due to mass loss in the supernova leads to efficient ejection of most enrichment candidates from their host clusters. Thus, most enrichment events occur shortly after the double neutron stars are born. This requires star-forming gas that can absorb the  $r$ -process ejecta to be present in the globular cluster 30–50 Myr after the initial burst of star formation. If scenarios for redistributing gas in globular clusters cannot act on these timescales, the number of neutron-star merger enrichment candidates drops severely, and it is likely that another mechanism, such as  $r$ -process enrichment from collapsars, is at play.

**Keywords:** globular clusters: general — methods:  $N$ -body simulations — stars: kinematics — binaries: close — stars: evolution — stars: neutron

### 1. INTRODUCTION

Astrophysical mechanisms for synthesizing the heaviest elements in the Universe are poorly understood, yet essential in explaining nucleosynthetic abundances observable today. Roughly half the elements heavier than iron are formed through the rapid capture of neutrons in a dense, neutron-rich environment, known as  $r$ -process nucleosynthesis (e.g., Cowan et al. 2019; Kajino et al. 2019). In these environments, the rate of neutron capture overcomes the rate of  $\beta$ -decay of radioactive nuclei, which converts the heavy nuclei into more stable isotopes with higher atomic numbers.

Once the prevalent paradigm, regular core-collapse supernovae (CCSNe) are now strongly disfavored both theoretically (Qian & Woosley 1996; Thompson et al. 2001; Roberts et al. 2012; Martínez-Pinedo et al. 2012) and observationally (Wallner et al. 2015; Hotokezaka et al. 2015) as a production site for heavy  $r$ -process elements. Furthermore, the discrepancy between the abundance spreads of Fe compared to heavy  $r$ -process elements such as Eu and La in the spectra of many metal-poor stars would be difficult to explain in the standard CCSNe  $r$ -process scenario, as such stellar explosions would likely introduce similarly high levels of Fe species into  $r$ -process enhanced stars (e.g., Ito et al. 2009; Placco et al. 2015). Specifically in the context of globular clusters (GCs), the homogeneous iron-group abundances and

\* zevin@u.northwestern.edu

inhomogeneous  $r$ -process abundances, as well as the fact that the internal spread of  $r$ -process elements is not correlated with light element dispersion, disfavors regular CCSNe as the production sites for  $r$ -process elements (Roederer 2011).

The neutron-rich ejecta from neutron-star mergers (NSMs) is theorized to fill these open gaps in the periodic table, polluting the universe with the heaviest naturally-occurring elements (Lattimer & Schramm 1974, 1976; Eichler et al. 1989; Meyer 1989; Davies et al. 1994; Ruffert et al. 1997; Rosswog & Liebend 1999; Freiburghaus et al. 1999). Over the last two decades, numerical simulations of the merger and post-merger phase have revealed numerous mechanisms by which neutron-rich material is ejected from these systems, including dynamical ejecta of tidal and shock-heated nature (Ruffert et al. 1997; Rosswog & Liebend 1999; Oechslin et al. 2007; Hotokezaka et al. 2013), neutrino-driven and magnetically driven winds from a (meta-)stable remnant (Dessart et al. 2009; Siegel et al. 2014; Ciolfi et al. 2017), and outflows from a post-merger accretion disk (Fernández & Metzger 2013; Just et al. 2015; Siegel & Metzger 2017). The fact that NSMs can indeed synthesize  $r$ -process elements was corroborated in August 2017 — the discovery of GW170817 and observations of the subsequent kilonova explosion (Abbott et al. 2017a) provided unequivocal evidence that NSMs are a site for heavy  $r$ -process nucleosynthesis (e.g., Chornock et al. 2017; Kasen et al. 2017; Tanvir et al. 2017). If NSMs are the main channel for heavy  $r$ -process enrichment (cf. Abbott et al. 2017b; Côté et al. 2017; Hotokezaka et al. 2018),  $r$ -process abundances in various astrophysical environments can thus probe the veiled physical mechanisms of binary stellar evolution, the rates of compact object mergers, and dynamical processes.

Globular clusters (GCs) are one intriguing environment where  $r$ -process enhanced, metal-poor stars have been observed, with a significant number of GCs exhibiting star-to-star dispersion of  $r$ -process species such as Eu and La (e.g., Sneden et al. 1997; Roederer & Sneden 2011; Roederer 2011; Sobeck et al. 2011; Worley et al. 2013). The tight correlation between the abundance ratios [La/Fe] and [Eu/Fe] indicate this enrichment is unlikely from  $s$ -process, since this would result in a much higher dispersion in [La/Fe] compared to [Eu/Fe] (Roederer 2011). Furthermore, measurements of [Pb/Eu] ratios also indicate that these clusters have negligible dispersion of  $s$ -process elements (e.g., Yong et al. 2006; Yong & Grundahl 2008; Sobeck et al. 2011; Roederer & Sneden 2011). Therefore, the astrophysical mechanism for introducing  $r$ -process elements must be inefficient at  $s$ -process production, or the dispersion of  $s$ -process elements is washed out from other, more frequent events.

From a sample of 11 GCs examined in Roederer (2011), 4 GCs showed clear signs of large  $r$ -process dispersion, 5 GCs showed no dispersion, and 2 GCs were more ambiguous with

smaller levels of dispersion. Though this sample is inadequate to make any definitive statements about the percentage of GCs that exhibit  $r$ -process enhancement, these numbers can be used as a rough estimate. Since this feature is apparent in a significant number of GCs but not ubiquitous across the full population, the mechanism for introducing  $r$ -process dispersion into these environments must occur in some, but not all, GCs.

These observations have a few immediate consequences. First, they indicate some kind of extended or secondary star formation episode early in the history of the GC, leading to stellar populations with distinct chemical abundances due to astrophysical processes that transpired over this time. Second, there must be an interstellar medium (ISM) in the young GC with a high enough density to reduce the energy and momentum from the relativistic  $r$ -process ejecta to prevent it from leaving the GC (Komiya & Shigeyama 2016). Third, to provide this dense ISM, there is likely a mechanism of replenish the natal GC environment with gas for forming a second generation of stars (such as AGB ejecta; Bekki & Tsujimoto 2017), as early-time SNe of massive stars will efficiently remove the natal gas embedded in the GC. Last, since GCs are believed to form the majority of their stars within the first 10–100 Myr after formation (for recent reviews on star formation episodes and the formation of multiple stellar populations in GCs, see e.g., Gratton et al. 2012; Bastian & Lardo 2018), the enrichment mechanism had to proceed on a relatively rapid timescale.

If NSMs are assumed to be responsible for the  $r$ -process enrichment in the second generation of stars formed in GCs, there are multiple stringent constraints on the properties of double neutron-star (DNS) systems at birth, most notably inspiral times and post-SN systemic velocities. Given the shallow gravitational potential expected of GC progenitors of the order of  $\sim 10 - 100 \text{ km s}^{-1}$  and small physical sizes of only a few pc, if the newly-formed DNSs attain appreciable post-SN systemic velocities they are typically ejected and must rapidly merge before fully evacuating the cluster environment. On the contrary, if newly formed NSs receive small enough kicks to remain in the cluster environment, they still must merge before the cluster is void of the gas that will form the second generation of (enriched) stars. This is also difficult, as the lower kicks will impart less eccentricity into the newly-formed DNS, resulting in a prolonged inspiral time. Dynamical interactions may also play a role in expediting NSMs in GCs (e.g., Grindlay et al. 2006; Lee et al. 2010), though once again these will need to have a significant impact early in the cluster lifetime. Though the NSM scenario for  $r$ -process enhancement has been explored in other environments such as ultra-faint dwarf galaxies (UFDGs; e.g., Safarzadeh et al. 2018), GCs provide a unique and complementary probe for investigating NSMs as the primary site

for *r*-process enrichment due to their vastly different physical sizes and masses, shorter star formation timescales, and the possible role of dynamical encounters.

In this paper, we examine multiple scenarios for rapid *r*-process enrichment in GCs using both of semi-analytic arguments and numerical modeling. In Section 2, we investigate NSMs produced by dynamical interactions, finding that this channel does not contribute to NSMs at early times. Section 3 examines the impact that compact binaries formed from isolated primordial stellar pairs could have on enrichment. We find that primordial binary evolution can only explain the observed *r*-process enrichment if systems are allowed to proceed through a phase of mass transfer (MT) involving a naked He-star donor. Though the stability of MT and survival of DNS progenitors during this phase is highly uncertain (Ivanova et al. 2003; Belczynski et al. 2008; Dominik et al. 2012; Tauris et al. 2015; Kruckow et al. 2016), we find that even if MT proceeds stably an appreciable number of NSM enrichment candidates are produced. In Section 4, we discuss the effect that MT and SNe prescriptions have on the enrichment candidates in our models, review the implication of our results on the properties of GC progenitors and star formation timescales, compare our results to other environments that have observed *r*-process enhanced stars, and suggest alternative scenarios that may lead to *r*-process enhancement in GCs. Finally, we highlight our main conclusions in Section 5.

## 2. DYNAMICAL ASSEMBLY OF DNS SYSTEMS

GCs host interesting and complex dynamics between stars and compact objects. Through dynamical friction, the most massive objects in a cluster sink to its core, where they readily take part in strong gravitational interactions. These interactions can induce rapid mergers of compact objects (e.g., Samsing et al. 2014; Rodriguez et al. 2016; Askar et al. 2017; Banerjee 2017; Giesler et al. 2018; Hong et al. 2018; Fragione et al. 2018; Rodriguez et al. 2018a; Zevin et al. 2018; Kremer et al. 2019b). However, via energy equipartition, as the most massive objects migrate to the cluster core, lighter objects move further away from the cluster center. As a consequence, black holes shape the dynamical evolution of the lower-mass ( $M \lesssim 1 M_\odot$ ) main sequence stars and, because these lighter stars make up the bulk of the total cluster mass, the cluster as a whole (e.g., Mackey et al. 2007, 2008; Kremer et al. 2018; Askar et al. 2018). At early times when a large black hole population is present, black holes therefore inhibit the dynamical segregation of the NSs that could potentially merge and enrich the cluster with *r*-process elements. Nevertheless, it has been argued that dense stellar environments such as nuclear star clusters in the early universe can yield an appreciable rate of dynamically-assembled NSMs and pos-

sible explain the *r*-process enhancement of metal-poor stars (Ramirez-Ruiz et al. 2015).

Over time, black holes will be ejected from the cluster through strong encounters with other black holes in the core (e.g., Spitzer 1987; Kulkarni et al. 1993; Sigurdsson & Phinney 1993; Morscher et al. 2015), allowing other lighter objects to follow suit and migrate toward the core through a similar segregation process, ultimately leading to cluster core-collapse (e.g., Kremer et al. 2019a). The depletion of black holes in the core also permits the segregation of NSs to the cluster core which leads to an increased formation rate of millisecond pulsars, DNSs and NSMs (Ye et al. 2019).

Mass segregation timescales can be approximated by the time necessary for a GC to settle into equilibrium. The half-mass relaxation time is given by

$$t_{\text{relax}} = 0.138 \frac{M_c^{1/2} R_h^{3/2}}{\langle m \rangle G^{1/2} \ln \Lambda}, \quad (1)$$

where  $M_c$  is the total cluster mass,  $\langle m \rangle$  is the average stellar mass,  $R_h$  is the half-mass radius, and  $\ln \Lambda$  is the Coulomb logarithm, where  $\Lambda \simeq 0.4N$  for GCs with  $N$  being the total number of stars (Spitzer 1987). For simple dynamical friction in a two-component model, the mass segregation timescale is

$$t_{\text{ms}}^i \sim \frac{\langle m \rangle}{m_i} t_{\text{relax}}, \quad (2)$$

where  $m_i$  is the mass of the segregating population (Spitzer 1987). For a typical cluster with  $M_c \simeq 4 \times 10^5 M_\odot$ ,  $\langle m \rangle \simeq 1 M_\odot$ ,  $R_h \simeq 1$  pc, and  $N \simeq 8 \times 10^5$ , the half-mass relaxation time is  $t_{\text{relax}} \simeq 100$  Myr (Meylan & Heggie 1997; Gurkan et al. 2004). Therefore, by Eq. (2),  $30 M_\odot$  black holes segregate in  $t_{\text{ms}}^{\text{BH}} \simeq 3 \times 10^6$  yr, whereas  $1 M_\odot$  neutron stars segregate in  $t_{\text{ms}}^{\text{NS}} \simeq 10^8$  yr.

To investigate this channel numerically, we model GCs using the Hénon-style Monte Carlo code, CMC (Hénon 1971a,b; Joshi et al. 2000, 2001; Fregeau et al. 2003; Pattabiraman et al. 2013; Chatterjee et al. 2010, 2013; Rodriguez et al. 2015). This code monitors and evolves the global properties of the GC via two-body relaxation, while accounting for binary stellar evolution (using updated versions of the SSE and BSE codes; Hurley et al. 2000, 2002) and small- $N$  gravitational encounters using the Fewbody package (Fregeau et al. 2004; Fregeau & Rasio 2007), which now includes post-Newtonian effects in  $N$ -body integrations (Antognini et al. 2014; Amaro-Seoane & Chen 2016; Rodriguez et al. 2018b). We record all strong encounters between objects, tracking the times at which new compact binary pairs are formed and calculating the gravitational-wave inspiral times of binaries synthesized due to these dynamical encounters.

We simulate two clusters — one with typical GC properties and one with a number of liberal assumptions in attempt to eliminate black holes from the environment so NSs will segregate to the cluster cores and interact as rapidly as possible.

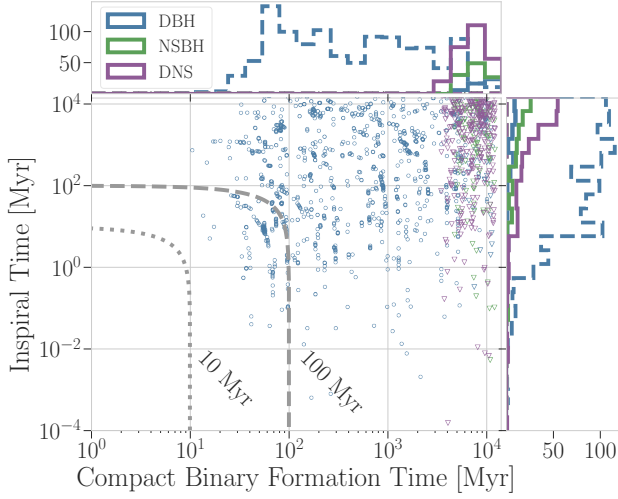


**Figure 1.** Inspirational times of compact binaries synthesized from dynamical interactions, relative to the time when the interaction occurred in the cluster. Dotted (dashed) gray lines are lines of constant time at 10 (100) Myr, the time at which we assume enrichment events must occur by; points that fall below and to the left of these lines merge before star formation ceases. Colored points and histograms indicate different classes compact object mergers: double black hole (DBH), neutron star-black hole (NSBH), and double neutron star (DNS). Circle (triangle) markers and colored dashed (solid) histograms show the distribution of mergers from the standard (liberal) model. Even in the liberal model where black holes are artificially removed, no NSMs occur before a few Gyr after cluster formation.

In this liberal model, we assume black holes have no mass fallback following the SN at their formation and receive full NS natal kicks and truncate the initial mass function (IMF) at  $20 M_{\odot}$  (which corresponds to a remnant mass of  $\sim 5\text{--}8 M_{\odot}$  at low metallicities; [Giacobbo et al. 2018](#)). This acts to reduce the number of black holes that are created from the initial stellar population, and efficiently eject those that do happen to form. Furthermore, we reduce all NS natal kicks, drawing their magnitude from a Maxwellian with a dispersion of  $20 \text{ km s}^{-1}$ . Figure 1 shows the time that compact binaries are dynamically formed in these models compared to their inspiral times. The sum of these two quantities approximates the time in the history of the cluster at which these compact binaries would merge, and in the case of systems with a NS component, possibly enrich the cluster with  $r$ -process material.

As expected, in the standard model binary black holes are the dominant dynamically-induced systems and inhibit the formation of other types of compact binaries for most of the GC lifetime. Only a small number of black holes merge within 100 Myr of the formation of the GC, and none merge within 10 Myr. Primordial mass segregation in star clusters

may help expedite dynamically-induced black hole mergers (e.g., [Parker 2018](#); [Alfaro & Román-Zúñiga 2018](#)), though the interaction rate of other types of compact objects will be stifled until the higher-mass black hole population is processed and ejected.

In our liberal model that artificially removes black holes and amplifies the number of retained NSs, we still do not find NS mergers until a few Gyr after cluster formation — far too late to enrich a second generation of stars with  $r$ -process material. Though black holes are efficiently removed from the cluster in this model, the  $1\text{--}2 M_{\odot}$  NS masses are still less massive than the subsiding main-sequence stars. Therefore, mass segregation is still inefficient for  $\sim 3$  Gyr until these stars finish their main sequence evolution. Though neutron star-black hole (NSBH) systems may also play a role in enrichment in our liberal model, the NSBH rate is lower than the DNS rate and they share similar inspiral time distributions, hence NSBH enrichment should be subdominant. We therefore conclude that *dynamical interactions in GCs do not contribute to early-time NSMs*, and therefore it is unlikely that dynamics plays a significant role enhancing second-generation GC stars with  $r$ -process.

### 3. MERGERS FROM PRIMORDIAL CLUSTER BINARIES

We next investigate the NSMs of primordial binaries following their isolated binary stellar evolution.<sup>1</sup> To pollute the cluster with  $r$ -process elements within the first  $\sim 10\text{--}100$  Myr after formation, DNSs must acquire short inspiral times through tight orbital separations and/or significant orbital eccentricities at birth. The standard picture by which compact binaries achieve hardened orbits during isolated binary evolution is via one (or more) common envelopes (CEs) — where one of the stars experiences Roche-lobe overflow (RLO) and unstable MT, enveloping both bodies in the outer layers of the donor star and exerting a drag on the orbiting binary system. This causes the binary to spiral inwards and harden its orbit (e.g., [Andrews et al. 2015](#); [Tauris et al. 2017](#); [Chruslinska et al. 2018](#)). For compact binaries that merge within a Hubble time, a CE phase will typically need to occur after one of the stars in the system has already evolved into a compact object so that the orbit can harden sufficiently without the bodies coming into contact and merging. Though the system circularizes following this evolutionary stage, eccentricity imparted into the system via the SN that forms the second NS will further reduce the gravitational-wave inspiral time.

<sup>1</sup> In this context, primordial binaries refer to stars that are born as binary pairs in the GC and have yet to segregate and undergo any dynamical interactions.



### 3.1. Enrichment efficiency

In addition to altering the orbital properties of the compact binary, the second SN can significantly kick the system through a combination of asymmetries in the explosion mechanism (the natal kick) and from mass-loss of the exploding star (the Blaauw kick; Blaauw 1961). The post-SN center-of-mass velocity is referred to as the systemic velocity. Given a final mass  $M_f = m_1 + m_2$  and initial mass  $M_i = m_1 + m_2 + \Delta M_{\text{SN}}$  where  $m_1$ ,  $m_2$ , and  $\Delta M_{\text{SN}}$  are the primary NS mass, secondary NS mass, and mass lost during the SN of the secondary, we can write the magnitude of the post-SN systemic velocity as

$$v_{\text{sys}}^2 = \frac{1}{M_f^2} \left[ (m_2 v_k)^2 + \frac{m_1 \Delta M_{\text{SN}} v_r}{M_f^2} (m_1 \Delta M_{\text{SN}} v_r - 2m_2 M_f v_{k\parallel}) \right], \quad (3)$$

where  $v_k$  is the magnitude of the natal kick,  $v_r$  is the relative orbital velocity between the two objects prior to SN, and  $v_{k\parallel}$  is the component of the natal kick aligned with the instantaneous orbital velocity of the exploding star (e.g., Kalogera 1996).

We consider DNS systems viable *r*-process polluters if the system merges within some enrichment radius of the cluster,  $R_{\text{enrich}}$ , and within the typical timescale of star formation in GCs,  $\Delta \tau_{\text{SF}}$ . This can happen in two general ways: (i) the post-SN systemic velocity is greater than the cluster escape speed, but the DNS merges before leaving the cluster environment and (ii) the post-SN systemic velocity is less than the cluster escape speed, and the DNS delay time is less than  $\Delta \tau_{\text{SF}}$ . To derive an approximate escape velocity, we assume the mass distribution in our fiducial clusters follow a Plummer profile (Plummer 1911):

$$\rho_p(r) = \left( \frac{3M_c}{4\pi R_p^3} \right) \left( 1 + \frac{r^2}{R_p^2} \right)^{-5/2}, \quad (4)$$

where  $M_c$  is the mass of the cluster and  $R_p$  is the Plummer radius. Given a Plummer radius, we assume DNS systems form at the half-mass radius, which is  $r_h \approx 1.3R_p$  for a Plummer sphere. The escape velocity is thus

$$v_{\text{esc}}(r_h) = \sqrt{2|\Phi_p(r_h)|} \approx 72 \left( \frac{M_c}{10^6 M_\odot} \right)^{1/2} \left( \frac{R_p}{1 \text{ pc}} \right)^{-1/2} \text{ km s}^{-1}, \quad (5)$$

where  $\Phi_p$  is the gravitational potential of the Plummer model. Though this is a simplistic description for the true potential of a young GC, we find our results to be robust to changes in the form of the potential since the post-SN systemic velocity of most enrichment candidates greatly exceeds the GC escape velocity.

Assuming negligible deceleration from the gravitational potential, if  $v_{\text{sys}} > v_{\text{esc}}$ , the time it takes for the DNS to go

beyond the enrichment radius of the cluster is

$$\tau_{\text{eject}} \approx \frac{R_{\text{enrich}}}{v_{\text{sys}}}. \quad (6)$$

We typically assume that the enrichment radius  $R_{\text{enrich}} = R_{\text{vir}} \approx 1.7R_p$  (e.g., Zwart et al. 2010), though later we will relax this assumption. Alternatively, systems that remain bound to the cluster after being kicked and merge within  $\Delta \tau_{\text{SF}}$  are also viable *r*-process polluters. The delay time is defined as  $t_{\text{delay}} = t_{\text{DNS}} + t_{\text{insp}}$ , where  $t_{\text{DNS}}$  is the time from zero-age main sequence (ZAMS) of the DNS progenitors to DNS formation and  $t_{\text{insp}}$  is the DNS inspiral time due to gravitational-wave emission (Peters 1964). We therefore categorize DNS systems that remain bound as viable polluters if  $t_{\text{delay}} < \Delta \tau_{\text{SF}}$ . Thus, the DNS enrichment efficiency is

$$\epsilon_{\text{DNS}} = \frac{1}{N_{\text{DNS}}} \sum_{i=0}^{N_{\text{DNS}}} \Theta(\Delta \tau_{\text{SF}}^i - t_{\text{delay}}^i) \times \mathcal{T}, \quad (7)$$

where  $N_{\text{DNS}}$  is the number of total number DNS systems,  $\Theta$  is the Heaviside step function, and  $\mathcal{T} = \Theta(\tau_{\text{eject}}^i - t_{\text{insp}}^i)$  if  $v_{\text{sys}} > v_{\text{esc}}$ , and  $\mathcal{T} = 1$  if  $v_{\text{sys}} \leq v_{\text{esc}}$ .

### 3.2. Neutron-star natal kicks

Proper motions of isolated pulsars in the Milky Way indicate that many NSs receive large natal kicks at birth on the order of a few hundred  $\text{km s}^{-1}$  (Fryer & Kalogera 1997; Hobbs et al. 2005; Bray & Eldridge 2018). As described above, the post-SN systemic velocity of DNS systems is affected by the natal kick, and it has been shown analytically that strong natal kicks can lead to systemic velocities that are  $\lesssim 50\%$  larger than the pre-SN orbital velocity (Kalogera 1996). Large natal kicks will more often disrupt the binary and therefore decrease DNS formation rates (Tauris & Takens 1998), though particular orientations and magnitudes of the natal kick, pre-SN orbital velocity, and mass loss in the SN can result in bound systems (Wex et al. 2002). Since the escape speeds of GCs are typically a few tens of  $\text{km s}^{-1}$ , DNSs in relatively tight pre-SN orbits that are not disrupted from standard CCSNe natal kicks will usually lead to post-SN systemic velocities that unbind the systems from their host cluster.

Evidence for some NSs receiving lower natal kicks has been determined by examining the proper motions of both the isolated NS population (Briskin et al. 2002) and galactic DNSs (Wong et al. 2010; Schwab et al. 2010; Beniamini & Piran 2016; Tauris et al. 2017). These lower kick magnitudes of a few tens of  $\text{km s}^{-1}$  are predicted for DNSs that explode due to electron capture in a strongly degenerate ONeMg core, known as electron-capture SNe (ECSNe; Miyaji et al. 1980; Nomoto 1984, 1987). ECSNe are typically assumed to occur when a star has a He core mass of around  $2 M_\odot$  at the base of

the AGB branch (cf. [Ivanova et al. 2008](#)), though the extent and placement of this range is debated ([Podsiadlowski et al. 2004](#)). This pathway will make it more likely for the DNS to remain bound to the cluster (as well as survive the SN), since lower natal kicks and smaller amounts of mass loss lead to smaller post-SN systemic velocities. However, the eccentricities imparted into the system from the SN will likewise be smaller, increasing the typical inspiral time.

In the models described in the following section, we therefore apply a bimodal distribution for natal kick magnitudes. Standard CCSNe have natal kicks drawn from a Maxwellian distribution with scale parameter  $\sigma_{\text{high}} = 265 \text{ km s}^{-1}$  ([Hobbs et al. 2005](#)), whereas for stars with He core masses at the base of the AGB branch in the range  $1.4 M_{\odot} \leq m_{\text{core}} \leq 2.5 M_{\odot}$ , which are predicted to undergo ECSNe ([Pfahl et al. 2002](#); [Podsiadlowski et al. 2004](#)), we draw natal kicks from a Maxwellian distribution with  $\sigma_{\text{low}} = 20 \text{ km s}^{-1}$ . Another possible mechanism for stifling natal kicks of DNSs is by significantly stripping the atmosphere of the progenitor star via binary interactions prior to the SN, a scenario known as ultra-stripped SNe (USSNe, [Tauris et al. 2013](#)), which we also take into account in one of our population models detailed below.

### 3.3. Population models

To determine  $\epsilon_{\text{DNS}}$ , we simulate multiple populations of merging DNSs using the COSMIC population synthesis code ([Breivik et al. 2019](#)).<sup>2</sup> COSMIC is a modified version of BSE ([Hurley et al. 2002](#)), which relies on polynomial fitting formulae for single stellar evolution ([Hurley et al. 2000](#)) and includes physical prescriptions for binary evolutionary processes such as tidal evolution, MT, CEs, and gravitational-wave decay ([Hurley et al. 2002](#)). COSMIC is updated to include state-of-the-art prescriptions for mass-loss in O and B stars ([Vink et al. 2001](#)), metallicity dependence in the evolution of Wolf-Rayet stars ([Vink & de Koter 2005](#)), new prescriptions for fallback and post-SN remnant masses ([Fryer et al. 2012](#)), variable prescriptions for the CE  $\lambda$  parameter ([Claeys et al. 2014](#)), as well as prescriptions for ECSNe ([Podsiadlowski et al. 2004](#)), USSNe ([Tauris et al. 2015](#)), and (pulsational) pair instability SNe ([Woosley 2016](#)). In addition, COSMIC determines when particular populations of compact binaries have been adequately sampled by repeatedly checking for convergence in the distributions of various binary properties ([Breivik et al. 2019](#)).

One aspect of binary evolution that we focus on in particular is the onset, stability, and outcome of MT that results from a post-He main sequence star overflowing its Roche lobe, known as Case BB MT ([Delgado & Thomas 1981](#); [Dewi et al. 2002](#); [Ivanova et al. 2003](#); [Tauris et al. 2013](#)). Case BB MT is believed to occur during the He-burning analog of the

Hertzsprung gap (HG), when core He burning has ceased and shell burning causes the star to expand. Initially, it was assumed that RLO from low-mass He stars that entered the HG was unstable and led to a successful CE phase ([Belczyński et al. 2002](#)), causing the spiral-in of the already-formed NS and the core of the He-star donor. Later, [Ivanova et al. \(2003\)](#) demonstrated with detailed stellar evolution simulations that most unstable MT during this evolutionary phase leads to delayed dynamical instability and merger, and for DNS progenitors the MT typically proceeds stably during He-shell burning. More recent work by [Tauris et al. \(2015\)](#) has confirmed this, and that the stability may be even more prevalent in DNS progenitors. This phase of binary evolution has important implications on fast-merging DNSs; Case BB MT is predicted to lead to the extremely hardened DNS systems at formation with orbital periods of  $\lesssim 10^{-2}$  days, which in the most extreme cases corresponds to inspiral times of  $\mathcal{O}(10^3)$  yr (e.g., [Vigna-Gómez et al. 2018](#)).

The five models we explore in this study cover a range of uncertainties in binary evolution by varying certain aspects of Case BB MT, the onset of CE evolution, survival through CEs, and natal kick prescriptions. In addition to providing astrophysically-motivated distributions of post-SN orbital properties and systemic velocities, they track the total sampled binary mass necessary to generate our population of DNSs. In all models we assume that all stars form in a single burst of star formation with a metallicity of  $Z_{\odot}/20$ :

- A) Standard BSE model, which allows for evolved He stars to proceed through a successful CE. NS masses are calculated using the Delayed prescription from [Fryer et al. \(2012\)](#).<sup>3</sup> For naked He stars, we adopt maximum mass ratios for stable MT from [Ivanova et al. \(2003\)](#):  $q_{\text{crit}} = 1.7$  for main sequence naked He stars (denoted as stellar type  $k_{\star} = 7$  in BSE) and  $q_{\text{crit}} = 3.5$  for HG or giant branch naked He stars ( $k_{\star} = 8, 9$ ). Other stellar types use the default BSE  $q_{\text{crit}}$  values.
- B) Same as Model A, except SNe that immediately follow a CE phase use the post-CE masses and orbital separations. By default, BSE uses the post-CE separation and pre-CE mass, which includes the mass of the ejected envelope. More details can be found in Appendix A.
- C) Same as Model B, except that unstable MT from donor stars without a well-developed core-envelope structure always lead to a merger. This is also assumed to be the case for donors in the HG, since they lack a clear entropy jump at the core-envelope boundary ([Ivanova & Taam 2004](#)). This is analogous to the pessimistic

<sup>2</sup> [cosmic-popsynth.github.io](https://cosmic-popsynth.github.io)

<sup>3</sup> Models run using the Rapid prescription from [Fryer et al. \(2012\)](#) only led to percent-level differences in our results.

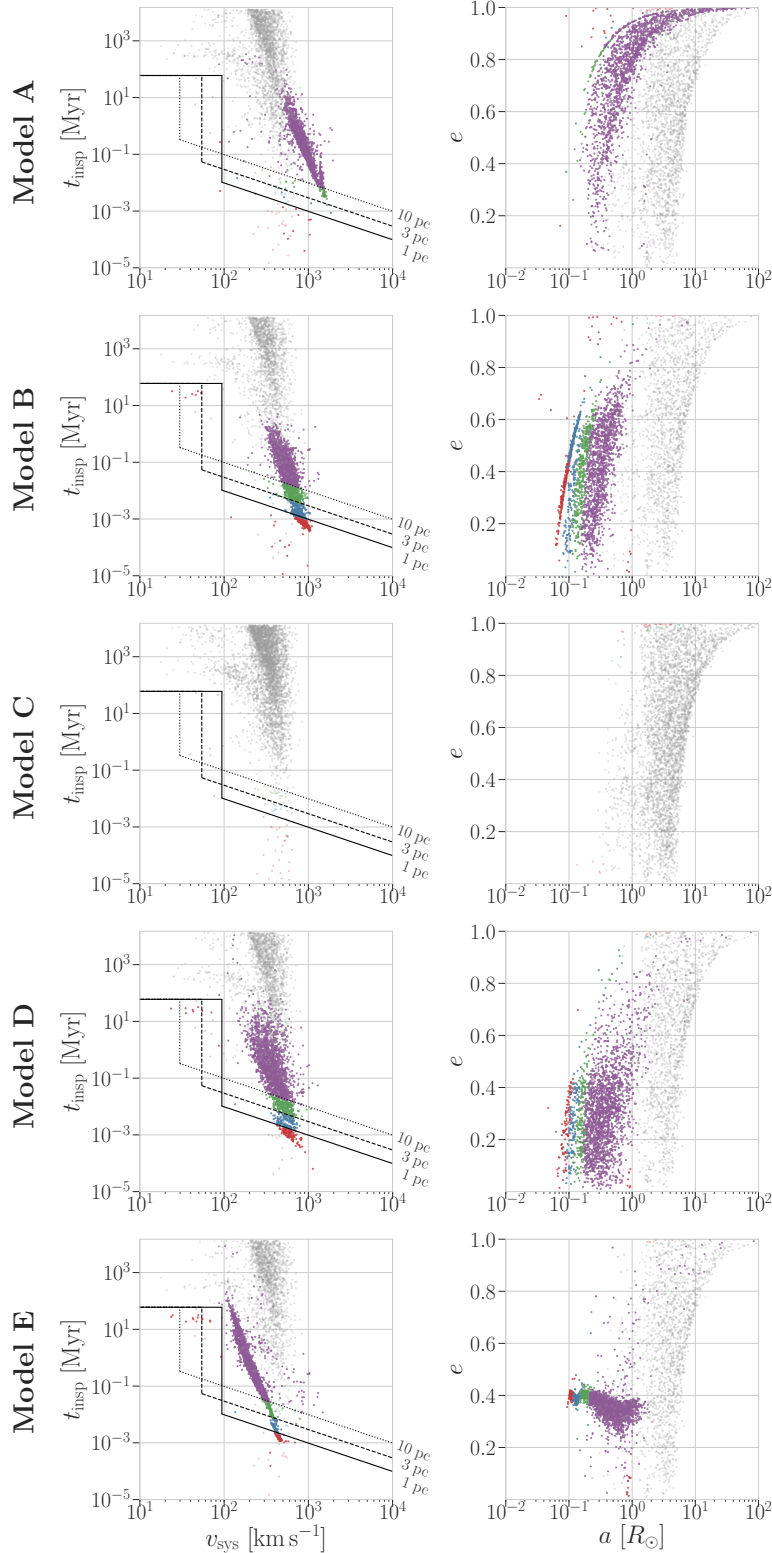


**Figure 2.** Post-SN properties of DNS systems that merge within a Hubble time from binary population synthesis models with varying assumptions (see Section 3.3 and Appendix A for details). Black lines distinguish systems that are enrichment candidates for three assumed cluster virial radii: solid, dashed and dotted correspond to 1 pc, 3 pc, and 10 pc, respectively. The diagonal component of the black lines marks a constant travel distance as a function of  $v_{\text{sys}}$ , the vertical black lines mark the cluster escape velocity (assuming a GC progenitor mass of  $10^6 M_{\odot}$ , and the horizontal black lines mark maximum inspiral time (assuming  $\Delta\tau_{\text{SF}} = 100$  Myr). Systems that fall below and to the left of the black lines are viable enrichment candidates assuming a virial radius of 1 pc (red), 3 pc (blue), and 10 pc (green), and are colored the same in both the left and right panels in a given row. For the remainder of the systems, purple points mark where the secondary star went through a stage of stable or unstable Case BB MT, and gray points mark systems where the secondary star went through only one CE.

CE model in Belczynski et al. (2008), and drastically limits the number of short-period systems since it eliminates potential DNS progenitors that would have otherwise gone through a phase of Case BB MT.

- D) Same as Model C, except orbital properties and mass-loss following MT with a He-star donor are calculated according to the fitting formulae in Tauris et al. (2015). The modeling in Tauris et al. (2015) finds that MY involving an evolved He-star donor typically proceeds stably and does not initiate a CE phase.
- E) Same as Model D, except all systems that undergo Case BB RLO are assumed to become ultra-stripped and receive the same natal kicks as ECSNe.

The time between ZAMS and DNS formation ( $t_{\text{DNS}}$ ) for our population of DNS ranges from  $\approx 11$ –68 Myr, with a median value of  $t_{\text{DNS}} = 41$  Myr. When calculating  $t_{\text{delay}}$  for an individual system, which factors into the DNS enrichment efficiency  $\epsilon_{\text{DNS}}$ , we use the  $t_{\text{DNS}}$  found from our modeling of that system, and integrate its post-SN semi-major axis and eccentricity according to Peters (1964) to determine  $t_{\text{insp}}$ .

#### 3.4. Enrichment fraction from primordial DNSs

Figure 2 shows the orbital properties immediately following the second SN for all DNSs that merge within a Hubble time in our population models, as well as the corresponding post-SN systemic velocity and inspiral times. Black lines separate DNS systems that are viable enrichment candidates (lower left) from those that either merge outside the cluster or after the star formation has ceased (upper right) for three assumed cluster sizes. Therefore, the enrichment fraction  $\epsilon_{\text{DNS}}$  from Eq. (7) is given by the fraction of systems that lie to the lower left of these lines. For the remainder of the population, systems that undergo a Case BB MT phase are colored in purple whereas those that proceed through only a single CE after the first NS formed (typically during the hydrogen giant branch of the secondary) are in gray. Systems that undergo Case BB MT provide the largest contribution to  $\epsilon_{\text{DNS}}$ , otherwise viable enrichment candidates can only result from systems that are kicked into an extremely eccentric orbit at birth (e.g., the small number of red points in Model C). However, as shown in Eq. (3), the post-SN systemic velocity scales with the orbital velocity of the binary prior to SN. Therefore, harder pre-SN binaries will have larger Blaauw kicks; this anti-correlation between systemic velocity and inspiral time for the Case BB systems is evident in Figure 2.

To calculate the fraction of GCs we expect to exhibit  $r$ -process dispersion, we must first determine whether a single NSM can distribute enough  $r$ -process material to enrich the stars in a GC. The total Eu mass of a GC can be roughly estimated by  $M_{\text{Eu}} \approx X_{\text{Eu},\odot} 10^{[\text{Eu}/\text{H}]} M_{\text{gas}}$ , where  $X_{\text{Eu},\odot}$  is the solar

Eu mass fraction and  $M_{\text{gas}}$  is the mass of intra-cluster gas in which the  $r$ -process was mixed into. For typical values, we have

$$M_{\text{Eu}} \approx 4.2 \times 10^{-5} \times 10^{[\text{Eu}/\text{H}]} \left( \frac{M_{\text{gas}}}{10^5 M_{\odot}} \right) M_{\odot}, \quad (8)$$

where we have used the solar abundances from Arnould et al. (2007), which amounts to  $\sim 4 \times 10^{-6} M_{\odot}$  assuming typical GC abundances from Roederer (2011). Assuming that a NSM can eject  $\approx 0.05 M_{\odot}$  of  $r$ -process material as in GW170817 (Cowperthwaite et al. 2017; Chornock et al. 2017; Kasen et al. 2017; Villar et al. 2017), which translates into a Eu mass of  $M_{\text{Eu}} \approx 5.2 \times 10^{-5} M_{\odot}$  assuming a solar abundance pattern starting at mass number  $A = 69$  (Arnould et al. 2007). We therefore conclude that a single NSM may be sufficient to enrich the second generation of stars in a typical GC.

Each model in Figure 2 is synthesized using a sample of binaries far larger than the stellar mass of a young GC. To quantify the typical number of NSMs that will pollute a single GC of mass  $M_c$ , we must multiply  $\epsilon_{\text{DNS}}$  by the mass fraction of stars that become DNSs, and scale this number by the typical stellar mass of a young GC. Since our models only simulate populations of binary systems, to convert to a total stellar mass we must also choose a reasonable initial binary fraction. Though over half of all high-mass stars in young stellar clusters are found in binary pairs (Sana et al. 2011), there is significant uncertainty in the initial binary fraction of high-mass stars in GCs (Ivanova et al. 2005). Since low-mass stars dominate the IMF,<sup>4</sup> we use a binary fraction in GCs of  $f_{\text{bin}} = 0.1$ , which is supported by observations of GCs (e.g., Rubenstein & Bailyn 1997; Bellazzini et al. 2002; Lucatello et al. 2015; Ji & Bregman 2015) and has been shown through numerical modeling to reproduce present-day binary fractions (Hurley 2007; Chatterjee et al. 2010). Therefore, the fraction of GCs that have an enrichment event from NSMs is

$$f_{\text{enrich}} = \epsilon_{\text{DNS}} N_{\text{DNS}} \frac{M_c f_{\text{bin}}}{M_{\text{samp}}}, \quad (9)$$

where  $M_{\text{samp}}$  is the total mass of binaries sampled in our population model. The enrichment fraction for our five population models using multiple assumptions for  $R_{\text{enrich}}$  and  $M_c$  are in Table 1.<sup>5</sup>

<sup>4</sup> Assuming a Kroupa IMF (Kroupa 2001) and a stellar mass range of  $0.05 M_{\odot} \leq M_{\star} \leq 300 M_{\odot}$ , stars above  $8 M_{\odot}$  only account for  $\sim 13\%$  of the total stellar mass.

<sup>5</sup> We do not consider NSBH mergers in our enrichment fraction calculations. The upper limit on the NSBH merger rate density measured by LIGO-Virgo is already lower than the median DNS merger rate density (Abbott et al. 2018). The mass fraction of binary stars that result in NSBH mergers should therefore be lower than that for DNSs, and therefore their enrichment contribution in GCs should be subdominant.



As anticipated, we find that enrichment fractions are sensitive to the assumptions made in population modeling. Notably, certain models (Models A and C) result in enrichment fractions that are far too low to be compatible with the *r*-process enhancement observed in GCs. Assuming NSMs are the primary mechanism for this enhancement, this provides a unique constraint on the intricacies of binary evolution that lead to DNSs. We discuss implications of each model's enrichment fraction in Section 4.1.

For a given population model, the enrichment fractions generally increase with increasing mass and cluster size. Increasing  $R_{\text{vir}}$  from 1 pc to 10 pc increases the enrichment fraction in most models by a factor of  $\approx 4$ . The enrichment fractions are typically  $\approx 2$  times larger for  $M_c = 10^6 M_\odot$  compared to  $M_c = 5 \times 10^5 M_\odot$ ; though the change in  $M_c$  affects the GC escape velocity, the primary contribution to  $f_{\text{enrich}}$  comes instead from the increased number of potential DNS progenitors, which scales linearly with  $M_c$ . However, as one pushes to extreme assumptions about the initial GC mass, this linearly scaling breaks down since many more DNSs remain bound to the natal GC. To this end, we also examined the enrichment fractions recovered when assuming an extreme assumption about the initial mass:  $M_c = 10^7 M_\odot$ . In this case, regardless of the cluster size, Models B, D, and E all have enrichment fractions greater than unity (i.e. all GCs would have at least one NSM enrichment event). However, Models A and C still can only achieve enrichment fractions of  $\lesssim 0.2$  at best.

The enrichment fractions in Table 1 assume that a NSM must occur within the virial radius of the young GC in order to enrich the still-forming second generation of stars. However, it may be possible to enrich the stellar populations from outside the cluster environment, though this will lead to a

		$R_{\text{vir}}$ [pc]		
		1.0	3.0	10.0
Model A	$5 \times 10^5$	0.3	0.4	1.0
	$10^6$	0.7	0.8	1.9
Model B	$5 \times 10^5$	3.6	8.0	12.7
	$10^6$	7.4	16.1	25.4
Model C	$5 \times 10^5$	0.2	0.2	0.3
	$10^6$	0.4	0.5	0.7
Model D	$5 \times 10^5$	1.5	3.2	6.1
	$10^6$	3.2	6.5	12.2
Model E	$5 \times 10^5$	1.2	2.5	4.8
	$10^6$	2.6	5.2	9.7

**Table 1.** Percentage of GCs that will have at least one enrichment candidate ( $100 \times f_{\text{enrich}}$ ) according to the various population models examined in Figure 2. The numbers in the table are for three representative sizes and two representative masses for the natal GC. In all cases,  $R_{\text{enrich}}$  is assumed equal to  $R_{\text{vir}}$ .

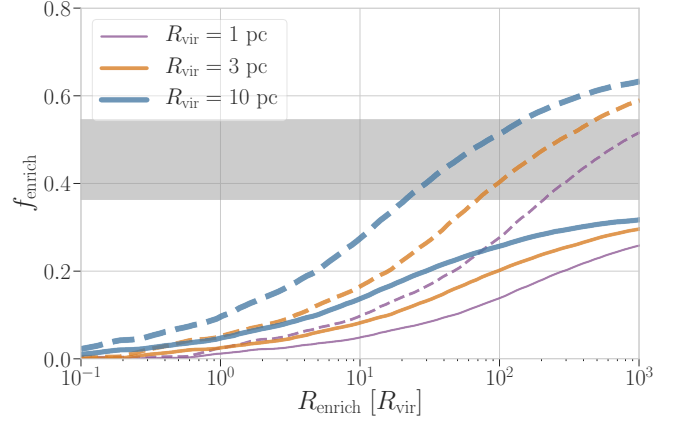


**Figure 3.** Enrichment fraction as a function of enrichment radius, in units of cluster virial radii, for DNS systems in Model E. The solid (dashed) line is for an assumed cluster masses of  $5 \times 10^5$  ( $10^6$ )  $M_\odot$ , and different colors represent different virial radii for the fiducial cluster. The gray shaded region marks the rough fraction of GCs with observed *r*-process dispersion from Roederer (2011); out of the 11 GCs in the catalog examined, 4 showed clear evidence of *r*-process dispersion, 2 were ambiguous with small dispersion, and 5 showed no signs of dispersion.

geometrical  $R^{-2}$  reduction of *r*-process material available for pollution, assuming the ejecta is isotropically dispersed. We examine  $f_{\text{enrich}}$  as a function of enrichment radius in Figure 3 for Model E. Enrichment fractions hit  $\sim 20\%$  at  $R_{\text{enrich}} = 10 R_{\text{vir}}$  and  $R_{\text{enrich}} = 100 R_{\text{vir}}$  for GCs with an initial mass of  $10^6 M_\odot$  and  $5 \times 10^5 M_\odot$ , respectively. Though even these liberal values for the enrichment radii still struggle to match the observed enrichment fraction in GCs, certain changes to our initial assumptions can ameliorate this tension. For example, since  $f_{\text{enrich}}$  scales linearly with the initial binary fraction, a higher initial binary fraction can act to increase these numbers further. However, Model C is incompatible with observations of enriched GCs regardless of the assumed enrichment radius and binary fraction, indicating that Case BB MT is necessary to explain *r*-process enhanced clusters in the NSM scenario.

#### 4. DISCUSSION

In the following sections, we highlight the implication of GC enrichment fractions on physical assumptions made about binary stellar evolution, discuss how initial properties and star formation timescales of GCs can be constrained by such observations, touch on other possible mechanisms for *r*-process enrichment in GCs, and comment on implications for other environments that have been observed to be *r*-process enhanced.

##### 4.1. *r*-process enrichment from primordial NSMs in GCs

Model A, which allows for successful CEs with an evolved He-star donor (Case BB CE), has enrichment fractions of

$\mathcal{O}(1\%)$ , well below the observed enrichment fraction of GCs ( $\sim 50\%$ ; Roederer 2011). Though the successful CE leads to hardened binaries that merge  $\lesssim 10$  Myr, the large systemic velocities of these DNSs cause them to escape the cluster environment before gravitational radiation causes them to inspiral and merge. However, in this standard BSE model the treatment of SN kicks immediately following a CE phase is not consistent, leading to systematically higher amounts of mass loss in the SN and amplified Blaauw kicks. This inconsistency strongly affects DNS post-SN orbital properties and inspiral times, and may also have a significant impact on DNS rates. Model A should therefore be considered as a fiducial model, for reference with regards to the standard behavior of BSE population modeling, rather than a plausible physical model. The treatment of mass loss and kicks is discussed further in Appendix A.

In Model B, we address this inconsistency by using the post-CE mass and post-CE separation when calculating the effect of SNe immediately after a CE event. This leads to systematically lower post-SN velocities and more DNSs surviving the second SN in general. Though the majority of DNS systems have post-SN systemic velocities greater than the escape velocity of the fiducial GCs, an appreciable number of DNS mergers still occur within the virial radii of the GC. Using our most liberal assumptions about the initial GC mass ( $M_c = 10^6 M_\odot$ ) and compactness of  $R_{\text{vir}} = 10$  pc, we find that the enrichment fraction reaches a value of  $\approx 25\%$ .

In Model C, which implements a pessimistic CE scenario as in Belczynski et al. (2008) and does not allow for CEs involving an evolved He-star donor, we find almost no enrichment candidates. Regardless of initial GC size and compactness,  $f_{\text{enrich}}$  is consistently  $\lesssim 10^{-2}$ ; the only enrichment candidates are those that proceed through a single CE are kicked into highly eccentric orbits from the second SN. This clearly shows that *without some form of Case BB MT, NSMs are unable to explain the r-process enhancement observed in GCs*.

Following Tauris et al. (2015), in Models D and E we assume that Case BB MT typically proceeds stably (i.e. Case BB MT does not lead to a CE phase). However, as the mass of the donor star is always greater than the mass of the first-born NS when considering DNS progenitors, stable MT will still cause the orbit to shrink. Since the orbital hardening is less drastic than if a CE occurred, we find lower enrichment fractions compared to Model B by a factor of  $\sim 2$  for Model D and  $\sim 3$  for Model E. The reason for lower enrichment fractions in Model E compared to Model D is the stifled natal kicks for systems that go through Case BB MT. This leads to less scatter in the post-SN orbital properties, a tighter trend in  $v_{\text{sys}}-t_{\text{insp}}$  space, and a slightly lower enrichment fraction.

Though the enrichment fractions for Models B, D, and E still fall slightly below the rough fraction of  $r$ -process en-

hanced clusters, we argue that, given the inherent uncertainty in a few of the parameters in our models, they are still consistent since they result in enrichment fractions that are order unity off from the observed values. For example, varying the initial properties of the natal GC affect these numbers; increasing  $R_{\text{vir}}$  increases the enrichment radius  $R_{\text{enrich}}$  while decreasing the escape velocity, and increasing  $M_c$  leads to a larger stellar mass available for forming DNSs while increasing the escape velocity. Furthermore, the enrichment fraction scales linearly with the initial binary fraction. Though we use  $f_{\text{bin}} = 10\%$  for our fiducial models, which is based on present-day GC observations, the initial binary fraction in GCs may have been higher (Ivanova et al. 2005). The choice binary fraction only affects the mass of the GC that goes into forming binaries; though the high-mass binary fraction may have even been 100%, it is the low-mass binaries that dominate the IMF and therefore contribute most to the binary mass sample. However, if the GCs had top-heavy IMFs (e.g., Marks et al. 2012; Kroupa & Jerabkova 2018), variations in the initial high-mass binary fraction will have a greater impact on the enrichment fraction. Regardless, Model C can still *never* match the observed enrichment fraction even with extremely liberal assumptions about the initial binary fraction and natal GC properties.

#### 4.2. Sensitivity to SN kicks and mass loss

Small natal kicks for some NSs at birth are necessary to explain the retention fraction of NSs in GCs (Pfahl et al. 2002). These retained systems are predicted to form from ECSNe or the accretion-induced collapse of a white dwarf (Ye et al. 2019). The retention of NSs formed in binary systems also depends on the Blaauw kick, which is anti-correlated with the square root of the binary orbital separation at the time of the SN.

As shown in Figure 2, most DNSs born as a binary pair have post-SN systemic velocities that would exceed the escape velocity of young GCs. This is particularly apparent for systems that undergo Case BB MT, as even small amounts of mass loss in their extremely hardened state prior to SN will result in post-SN systemic velocities of  $\gtrsim 100 \text{ km s}^{-1}$ . This does not conflict with the number of pulsars observed in GCs today since isolated NSs do not receive a Blaauw kick at formation — the natal kick alone controls the post-SN velocity and therefore whether or not it remains bound to the cluster.

Hardened DNS systems that underwent Case BB MT make up the bulk of the systems that contribute to  $f_{\text{enrich}}$ . In their tight orbital configurations, the natal kick is typically small compared to the pre-SN orbital velocity, and the post-SN systemic velocity is mostly controlled by the mass lost in the SN rather than the natal kick that the exploding star received (Kalogera 1996). Lower amounts of mass loss in the SN could therefore lead to more of these systems being retained,

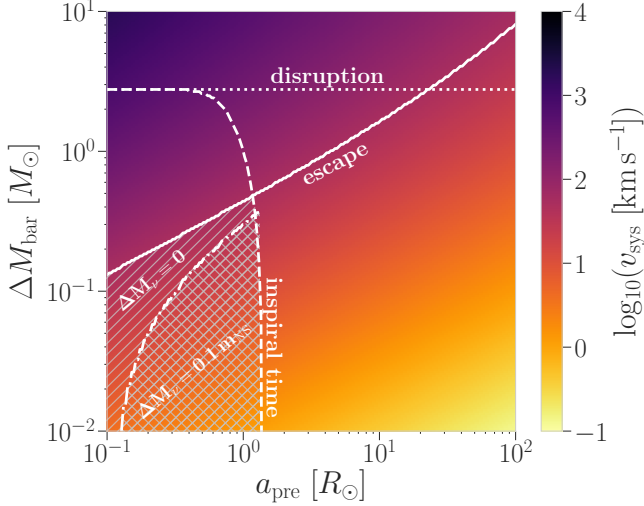


**Figure 4.** Viable enrichment candidates from DNS systems which remain bound to the GC. We solely examine the effect of the Blaauw kick from mass loss in the SN;  $v_{\text{sys}}$  is the post-SN systemic velocity assuming the natal kick is zero.  $\Delta M_{\text{bar}}$  is the baryonic mass loss, such that the total mass lost in the SN is  $\Delta M_{\text{SN}} = \Delta M_{\text{bar}} + \Delta M_{\nu}$  with  $\Delta M_{\nu}$  being the mass loss from neutrinos due to the collapse of the stellar core into a NS. NS masses of  $m_{\text{NS}} = 1.4 M_{\odot}$  are assumed for both components. The solid white line marks the escape velocity from the half-mass radius of a GC progenitor with  $M = 10^6 M_{\odot}$  and  $R_p = 3$  pc. The dashed white line marks an inspiral time of 100 Myr. Systems that satisfy these two criteria fall below and to the left of these two lines (in the white hatched region) and are viable enrichment candidates that remain bound to the GC. The diagonal hatched region assumes that  $\Delta M_{\nu} = 0$ , i.e. there is no neutrino mass loss. The dot-dashed line and cross-hatched region assume that  $\Delta M_{\nu} = 0.1 m_{\text{NS}}$ , further constraining the possible combinations of  $\Delta M_{\text{bar}}$  and  $a_{\text{pre}}$ . Systems above the dotted white line are disrupted due to losing over half their total mass.

thereby amplifying the number of enrichment candidates (i.e. moving the purple points in the left column of Figure 2 to the left).

In Figure 4 we show the impact of mass loss in the SN and pre-SN separation on the post-SN systemic velocity. For simplicity, we assume the natal kicks are zero and both NSs have a mass of  $m_{\text{NS}} = 1.4 M_{\odot}$ , such that the post-SN systemic velocity reduces to an exact expression that is solely dependent on the orbital separation and mass loss:

$$v_{\text{sys}}|_{v_k=0} = \frac{\Delta M_{\text{SN}}}{2} \sqrt{\frac{G}{a_{\text{pre}}(2m_{\text{NS}} + \Delta M_{\text{SN}})}}. \quad (10)$$

The entire hatched region marks the pre-SN separations and mass loss that forms a DNS that is bound to the cluster and merges within 100 Myr. Stable Case BB MT can deplete the envelopes of the donor stars such that the mass loss in the subsequent SNe can be as low  $\sim 0.1 M_{\odot}$  and harden pre-SN orbits to  $a_{\text{pre}} \lesssim 1 R_{\odot}$  (Tauris et al. 2015), safely within the hatched region. However, regardless of the level at which the

envelope of the donor star is stripped, mass loss from neutrinos during the collapse of the stellar core can lead to a non-negligible contribution to the systemic velocity of the post-SN binary (Lattimer & Yahil 1989; Lovegrove & Woosley 2013). The dot-dashed line further constrains the parameter space by assuming 10% of the NS mass is lost in neutrino emission during the SN; under this assumption bound systems that are viable enrichment candidates only reside in the narrow cross-hatched region of parameter space.

Fortuitous orientations of the natal kick can increase the parameter space that will lead to DNSs with low enough systemic velocities such that they remain bound to the cluster. However, assuming isotropic natal kicks, this will only happen for a small number of DNS systems. Given how fine-tuned these conditions must be, we expect the  $f_{\text{enrich}}$  contribution of bound, fast-merging DNSs to be small regardless of the physical prescriptions underlying Case BB stripping, with the bulk of the enrichment candidates coming from DNSs that are unbound from the cluster and merge before evacuating the cluster environment.

#### 4.3. Common envelope prescriptions for Hertzsprung gap He stars

As seen in Figure 2, the vast majority of viable enrichment candidates proceed through a phase of Case BB MT. However, the ability for binary systems to proceed through this phase is highly uncertain. Dynamical instability during RLO may lead to merger for stars without a core-envelope structure or a clear entropy jump at the core-envelope transition (Ivanova & Taam 2004; Belczynski et al. 2008). Model C enforces this, causing all stars that undergo unstable MT during these phases of stellar evolution to merge, eliminating the Case BB systems and thereby depleting the population of systems with short inspiral times and viable enrichment candidates. Without Case BB MT, systems seldom have the ability to enrich GCs; only extremely hardened systems that get kicked into eccentricities near unity merge quick enough and within the cluster environment, which would only be able to explain star-to-star  $r$ -process dispersion in  $\sim 0.1$ – $1\%$  of clusters.

First pointed out by Ivanova et al. (2003) and more recently investigated in detail by Tauris et al. (2015), RLO between a naked He-star donor with a neutron-star companion typically proceeds stably if DNS systems are to form, thereby avoiding a second CE and subsequent merger. In addition, Vigna-Gómez et al. (2018) found that populations where this phase of MT typically proceeds stably are in better agreement with the Milky Way DNS population than models that allow for Case BB CEs.

Tauris et al. (2015) provided fitting formulae that map pre-RLO masses and separations to their values following RLO (i.e. the values immediately prior to the SN) from their mod-

els that find this phase of MT to typically proceed stably.<sup>6</sup> In Models D and E, we pause our binary evolution at the onset of He-star RLO and implement these fitting formulae to determine the pre-SN masses and separations. These models lead to slightly lower post-SN systemic velocities than the models which allow for the onset of Case BB CEs; in Model B the median post-SN systemic velocity for systems that undergo Case BB MT is  $\sim 600 \text{ km s}^{-1}$ , whereas Models D and E have median systemic velocities of  $\sim 400 \text{ km s}^{-1}$  and  $\sim 200 \text{ km s}^{-1}$ , respectively. Though these systems are less likely to be ejected, as seen in Figure 2 the majority would still exceed the escape velocity of a fiducial GC. Furthermore, Case BB systems in Models D and E have slightly longer inspiral times, which leads to slightly lower enrichment fractions than in the case where Case BB MT proceeds unstably. This is particularly evident in Model E, where Case BB donors are assumed to be ultra-stripped and have stifled natal kicks. In Model B, 73% of systems that went through Case BB MT have inspiral times less than  $10^5 \text{ yr}$ , whereas this number drops to 41% and 27% for Models D and E, respectively.

Overall, significant hardening of the pre-SN binary has a counteractive effect on the enrichment efficiency. Though hardened pre-SN orbits typically lead to shorter inspiral times, they also amplify post-SN systemic velocities; even if the natal kicks are small, high post-SN systemic velocities will be achieved through Blaauw kicks (Kalogera 1996). This causes hardened systems to be more easily ejected from the GC. Larger pre-SN orbital separations will reduce the effect of the Blaauw kick, but will also increase the inspiral time. In the context of GCs, enrichment candidates are typically in the first of these regimes: ejected from the GC but residing in the tail of the inspiral time distribution such that they merge before leaving the GC entirely.

#### 4.4. Initial cluster properties

The GCs with observed  $r$ -process dispersion have varying properties; both core-collapsed and non-core-collapsed clusters show dispersion, and present-day masses of these clusters range from  $\sim 2 \times 10^5 - 5 \times 10^5 M_\odot$  (Kimmig et al. 2015; Boyles et al. 2011; Leonard et al. 1992). However, since most of the Milky Way’s GCs formed  $\sim 10 \text{ Gyr}$  ago, initial GC properties are highly uncertain. Observations of super star clusters, which are believed to be the progenitors of GCs, help to elucidate the initial conditions of these old stellar systems. These observations indicate that the stellar masses of GCs found in the Milky Way today are a factor of a few to more times less massive than they were at formation (e.g., Leroy et al. 2018), and in some extreme cases

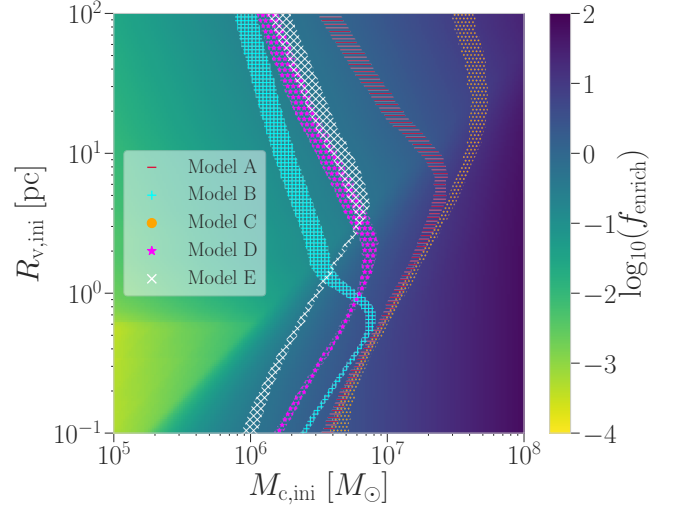


**Figure 5.** Mapping of enrichment fractions to initial GC properties, assuming a single NSM within the virial radius of the young GC is required for enrichment. Population Model E is used for determination of the  $f_{\text{enrich}}$  colormap. The various hatched regions indicate the constraints on initial cluster properties for different population models, assuming the approximate range of  $f_{\text{enrich}}$  from the sample of GCs examined in Roederer (2011). Due to their limited ability to enrich the fiducial GCs, Models A and C push to much more extreme initial cluster properties.

super star clusters can reach masses of  $\sim 10^7 M_\odot$  (Herrera & Boulanger 2017; Vanzella et al. 2017).

More massive natal GCs lead to more enrichment candidate NSMs due to deeper gravitational potentials (higher escape velocities) and, more importantly, more stars sampled from the IMF that can potentially form DNS binaries. In our analysis, we investigated two representative natal GC masses of  $5 \times 10^5$  and  $10^6 M_\odot$ . These assumptions are corroborated by numerical studies that find most present-day GCs to be a few times more massive at birth (e.g., Webb & Leigh 2015). However, if working under the assumption that a particular DNS population is the true representation of DNSs in young GCs and that NSMs are the sole contributor to  $r$ -process enhancement in GCs, the inference can be reversed to place constraints on initial conditions of GCs needed to match the number of enriched GCs. Figure 5 demonstrates this by highlighting the regions of initial cluster mass–initial cluster size space that lead to the observed enrichment fraction in our population models; the hatched regions represent the fraction of GCs with star-to-star  $r$ -process dispersion according to the sample from Roederer (2011).

Assuming the enrichment event must occur within the virial radius of the cluster, this maps to typical GCs with a physical size of  $\sim 3 \text{ pc}$  (10 pc) and stellar masses of  $\sim 5 \times 10^6$  ( $2 \times 10^6$ )  $M_\odot$  at formation. Though this is  $\approx 10$  times more massive than the present-day masses of the GCs with observed  $r$ -process dispersion, simulations of massive star clus-

<sup>6</sup> Though further phases of stellar evolution occur before the SN, they proceed on rapid timescales and any stable or unstable MT will not strongly affect the orbital properties of the pre-SN system.



ter formation do find stellar masses of up to  $\approx 1\text{--}2 \times 10^6 M_\odot$  (Tsang & Milosavljević 2018, see also Skinner & Ostriker 2015; Raskutti et al. 2016). However, the constraints on initial cluster masses from our modeling should be taken with caution, since many other uncertain factors (e.g., the initial binary fraction of stars) could also reconcile the slightly low  $f_{\text{enrich}}$  values in these models. As of now, the theoretical uncertainties in the evolution of DNS progenitors currently prohibit any definitive statements about initial GC properties. If future observations of DNSs in both the Milky Way and via gravitational waves can further constrain uncertain aspects of high-mass binary stellar evolution, the enrichment fraction observed in GCs could help probe the uncertain initial properties of GC progenitors.

#### 4.5. Extended star formation in young GCs

The timespan over which star formation occurs in GCs is uncertain, though typically believed to be  $\mathcal{O}(10)$  Myr (Gratton et al. 2012; Bastian & Lardo 2018). The primary drivers of this time constraint are radiation pressure and feedback from the SNe of high-mass stars, which proceed through the entirety of their stellar evolution in only a few Myr. However, other mechanisms have been proposed for redistributing gas within young GCs, which needs to be sufficiently dense to halt the relativistic *r*-process ejecta from NSMs and to form new, *r*-processed enhanced stars. For example, Bekki & Tsujimoto (2017) suggest that this may be accomplished through the conglomeration of AGB ejecta from  $6\text{--}9 M_\odot$  stars, which can form a high-density compact gaseous region in the center of a young GC. This gas would begin to pollute the cluster  $\sim 100$  Myr after the initial burst of star formation, after the removal of gas chemically polluted by the SNe of high-mass stars.

We take a conservative star formation timescale of 100 Myr for most of the values presented in this paper, which is corroborated by observations of young massive star clusters (Vanzella et al. 2018). Though the free-fall timescale of a  $10^6 M_\odot$  molecular cloud about 10 pc in radius is only  $\approx 1$  Myr, star clusters in general do not form from one single isolated cloud but rather through the hierarchical merging of smaller clusters. In this more realistic picture where clusters form hierarchically in turbulent molecular clouds with free-fall times of tens of Myr, it is not unreasonable for new star formation to occur  $\approx 100$  Myr into the cluster evolution as gas clouds continue to stream down the potentials of the newly formed clusters. Nonetheless, our results are largely insensitive to increases in this number; as seen in Figure 2, few systems fall directly above the horizontal black line at  $t_{\text{insp}} = 100$  Myr, so increasing  $\Delta\tau_{\text{SF}}$  has little impact on  $\epsilon_{\text{DNS}}$ . For example, assuming a progenitor GC mass of  $10^6 M_\odot$  and virial radius of 3 pc, increasing  $\Delta\tau_{\text{SF}}$  from 100 Myr to 1 Gyr increases the enrichment fraction by 1.2%, 4.6%, and 3.8%

in Models B, D, and E, respectively. Therefore, cluster formation scenarios that invoke more extended star formation episodes will not lead to an amplification of enrichment candidates.

In contrast, results can change drastically if we decrease  $\Delta\tau_{\text{SF}}$ . In Figure 6, we show the enrichment fraction as a function of  $\Delta\tau_{\text{SF}}$  for various assumptions on the properties of the natal GCs. Regardless of the properties of the GC,  $f_{\text{enrich}}$  plateaus at  $\approx 40$  Myr, which is the median formation time of DNS systems in our models. For example, a value of  $\Delta\tau_{\text{SF}} = 30$  Myr produces only  $\approx 4\text{--}7\%$  of the enrichment candidates as  $\Delta\tau_{\text{SF}} = 50$  Myr across our population model. This is because the evolutionary timescales of DNS progenitors typically exceed  $\Delta\tau_{\text{SF}}$  for  $\Delta\tau_{\text{SF}} \lesssim 30$  Myr.

The steep buildup of  $f_{\text{enrich}}$  at 30–50 Myr has important implications for *when* the redistribution of gas in the GC must have occurred by. Since most of the DNS mergers that contribute to enrichment are those that are ejected from the GC at formation and quickly merge, NSMs that are viable enrichment candidates must merge shortly after DNS formation. Therefore, for NSMs to be a viable scenario for *r*-process enhancement, star formation in GCs *must* be ongoing or rejuvenated at the time that DNSs form,  $\approx 40$  Myr after the initial burst of star formation. This criteria may be hard to accomplish using, for example, lower-mass AGB stars as the mechanism for re-polluting the GC with gas  $\approx 100$  Myr after formation, and may indicate that another mechanism for *r*-process enhancement in young GCs is at play.

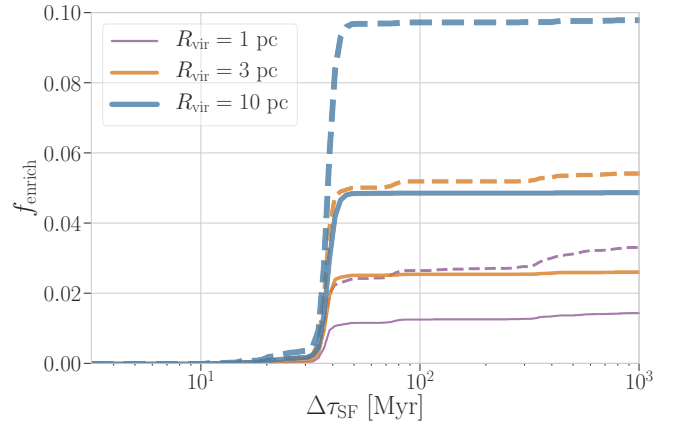


**Figure 6.** Enrichment fraction as a function of the timescale of star formation in a young GC. The solid (dashed) lines are for an assumed cluster mass of  $5 \times 10^5$  ( $10^6$ )  $M_\odot$ , and different colors represent different virial radii for the fiducial cluster. Model E is used in this figure; though different models lead to different peak values of  $f_{\text{enrich}}$ , the steep build-up of  $f_{\text{enrich}}$  occurs at the same point in all models, as this is primarily determined by the stellar lifetime of DNS systems. The plateau of  $f_{\text{enrich}}$  at values of  $\Delta\tau_{\text{SF}} \gtrsim 50$  Myr is due to most enrichment candidates being rapidly-merging DNS systems that are unbound from their host cluster.

#### 4.6. Alternative scenarios for enrichment

As demonstrated in the above sections, the NSM scenario for  $r$ -process enrichment is broadly compatible with the observed number of enriched GCs if star formation for forming the second generation of stars is ongoing at to time of DNS formation,  $\approx 30$ – $50$  Myr after the initial bout of star formation. Though this may be possible, either through extended star formation or a redistribution of gas from stellar processes after the first wave of SNe heat and eject the natal gas, other scenarios that can contaminate the cluster with  $r$ -process material at early times may also be viable.

Various other astrophysical scenarios have been proposed for contributing to the observed abundances of  $r$ -process elements (see [Kajino et al. 2019](#), for a review). One such scenario is via the formation of a dense accretion disk during the collapse of a massive, rapidly-rotating star — the *collapsar* scenario ([Woosley 1993](#); [Siegel et al. 2019](#); [Siegel 2019](#)). This scenario has also been suggested to be the cause of long  $\gamma$ -ray bursts (GRBs; e.g., [MacFadyen & Woosley 1999](#)). Collapsars arguably better satisfy existing constraints on  $r$ -process enrichment and may overcome problems or alleviate tensions that enrichment scenarios solely based on NS mergers face (see [Siegel 2019](#) for a brief discussion on some of the issues). This relates to issues of prompt enrichment at low metallicities (e.g., [van de Voort et al. 2015](#); [Shen et al. 2015](#); [Wehmeyer et al. 2015](#); [Cescutti et al. 2015](#)), and also to the high-metallicity stars of the Milky Way disk (e.g., [Hotokezaka et al. 2018](#); [Siegel et al. 2019](#); [Côté et al. 2019](#)). Though potential concerns have been raised regarding the co-production of iron in the context of extremely metal-poor stars ([Macias & Ramirez-Ruiz 2019](#)), this may not be applicable to  $r$ -process enrichment in GCs; given the total mass and metallicity of GCs that show internal  $r$ -process dispersion, many SNe likely occurred in young GCs.

Unlike enrichment from merging DNSs, the collapsar scenario is not susceptible to ejection from the GC due to large post-SN systemic velocities. Furthermore, as collapsars result from massive star evolution, they could occur within a few Myr of the initial burst of star formation, when natal gas is still present in the cluster environment and the first wave of stars are still forming. However, for this scenario to be viable, the rate density of collapsars per unit of stellar mass must be in line with the total stellar mass available to the young GC.

By assuming collapsars are the cause of long GRBs, the number of collapsars per unit stellar mass formed can be empirically estimated from the observed local long GRB rate. Assuming that the rate of collapsars (events per unit comoving volume per unit time) tracks the star formation rate  $\rho_{\text{SF}}$  (stellar mass per unit comoving volume per unit time) with negligible delay ( $\sim$  few Myr),  $R_{\text{coll}}(t) \propto \rho_{\text{SF}}(t)$ , where  $t$  denotes cosmic time. Thus, one can write the total number of

collapsars per unit stellar mass formed as

$$n_{\text{coll}} = \frac{\int R_{\text{coll}}(t) dt}{\int \rho_{\text{SF}}(t) dt} = \frac{R_{\text{coll}}(z=0)}{\rho_{\text{SF}}(z=0)}. \quad (11)$$

The collapsar rate is given by  $R_{\text{coll}}(z=0) = R_{\text{LGRB}}(z=0)/f_b$ , where  $R_{\text{LGRB}}(z=0) \approx 1.3^{+0.6}_{-0.7} \text{ Gpc}^{-3} \text{ yr}^{-1}$  is the rate of local ( $z=0$ ) long GRBs ([Wanderman & Piran 2010](#)) and  $f_b \approx 5 \times 10^{-3}$  is the GRB beaming fraction ([Goldstein et al. 2015](#)). This GRB rate does not include the separate class of low-luminosity GRBs ([Liang et al. 2007](#)), which likely produce only little to no  $r$ -process material at all ([Siegel et al. 2019](#)). Employing the cosmic star formation history as reported by [Madau \(2017\)](#), we obtain from Eq. (11):

$$n_{\text{coll}} = 2.6^{+1.2}_{-1.4} \times 10^{-5} \left( \frac{f_b}{5 \times 10^{-3}} \right)^{-1} M_{\odot}^{-1}. \quad (12)$$

This estimate also roughly applies to collapsars in our Milky Way.

The estimate in Eq. (12) is unchanged when considering that collapsars and GRBs may only occur up to a certain metallicity threshold. Host galaxy studies of long GRBs show that they preferentially occur below a certain stellar metallicity and thus may have shut off in recent Galactic history ([Stanek et al. 2006](#); [Perley et al. 2016](#)). The metallicity threshold for collapsars is slightly sub-solar, and is thus not of relevance at the metallicities of old, metal-poor GCs considered here. Assuming that the estimate Eq. (12) also roughly applies to star formation in GCs, this would indicate that given typical initial GC masses of  $5 \times 10^5 M_{\odot}$  to  $10^6 M_{\odot}$ , most young GCs could have of order unity collapsar events early in their cosmic histories. As collapsars tend to produce more  $r$ -process material per event than NSMs ([Siegel et al. 2019](#)), a single collapsar event per GC may be enough to explain the observed internal  $r$ -process dispersion of GCs (see Sec. 3.4). This simple estimate thus indicates that collapsars may indeed be a viable  $r$ -process enrichment scenario for GCs. Future work, however, is required to provide a better quantitative estimate, which is beyond the scope of this paper. One open question is whether a collapsar event early in the GC's history can lead to sufficient inhomogeneity of its  $r$ -process ejecta into a new generation of stars to explain the observed dispersion in  $r$ -process elements. While this seems conceivable at first sight, future work is needed to address this question quantitatively.

Finally, MHD supernovae ([Winteler et al. 2012](#); [Thompson et al. 2004](#); [Metzger et al. 2008](#)) might provide another source of  $r$ -process enrichment. If MHD supernovae indeed occur at a rate of 0.1–0.3% of CCSNe as assumed by [Wehmeyer et al. \(2015\)](#), we obtain in analogy to Eq. (11)  $n_{\text{MHDNS}} \approx (7 \times 10^{-6} - 2 \times 10^{-5}) M_{\odot}^{-1}$ , i.e., again order unity enrichment events per GC. Here, we have used the observed local CCSN rate of  $7.05^{+1.43}_{-1.25} \times 10^{-5} \text{ Mpc}^{-3} \text{ yr}^{-1}$  ([Li et al. 2011](#)). However, when

considering the three-dimensional stability of the magnetized jets that give rise to the fast-expanding neutron-rich ejecta in these systems (Mösta et al. 2014), such events are challenged to eject significant amounts of heavy *r*-process nuclei (Mösta et al. 2018; Halevi & Mösta 2018). Additionally, if MHD supernovae did produce significant amounts of heavy *r*-process elements, the high opacity of the lanthanide material would be mixed with the  $^{56}\text{Ni}$  of the supernova ejecta in a way that would likely be incompatible with present observations of CCSNe (Siegel et al. 2019).

#### 4.7. *r*-process enrichment in other environments

Enhancement of *r*-process material in metal-poor stars has been observed in various other environments, including UFDGs Ji2016, Hansen2017 and the galactic halo (Hansen et al. 2018; Sakari et al. 2018). Similar to GCs, the enhancement in UFDGs is difficult to explain using the NSM scenario due to their shallow gravitational potential, and depends strongly on kicks and distance traveled prior to merger (e.g., Andrews & Zezas 2019). Even with low kick velocities for DNS systems, the extremely shallow gravitational potentials of UFDGs lead to NSMs that are typically at large offsets from their hosts (Bonetti et al. 2019).

Using the population synthesis models from Dominik et al. (2012), which use the *StarTrack* code (Belczyński et al. 2002), Safarzadeh et al. (2018) found that the only way NSMs can explain the enrichment in the UFDG Tucana III is if they proceed through unstable Case BB MT and form extremely hardened DNSs that merge before its post-SN systemic velocity causes it to evacuate the UFDG. However, the modeling in Safarzadeh et al. (2018) still found it difficult to explain the enrichment in Reticulum II from this scenario. From our population models, we find a similar tension in the NSM enrichment scenario for UFDGs; for Tucana III-like and Reticulum II-like initial stellar masses and  $r_{\text{vir}} \approx 4.5$  kpc, we find that  $\approx 6\%$  and  $\approx 1\%$  of Tucana III-like and Reticulum II-like UFDGs would have an NSM enrichment event, respectively. This is in contrast with the  $\approx 20\%$  of UFDGs that are *r*-processed enhanced. These numbers are nearly identical whether or not unstable (Model B) or stable (Models D and E) Case BB MT is assumed; the reason that unstable Case BB models produce about double the enrichment candidates than stable Case BB models in GCs is due to the small physical sizes (and therefore the necessity for short inspiral times to merge before ejection) of GCs compared to UFDGs. This indicates that if the NSM scenario is the main contributor to *r*-process enhancement in UFDGs the onset of Case BB CEs is not necessary, which is in better agreement with studies that find this phase of MT to typically proceed stably (Tauris et al. 2015; Vigna-Gómez et al. 2018).

## 5. CONCLUSIONS

In this study, we examine the efficiency of NSMs at enriching young GCs with *r*-process material. The enrichment mechanism must occur relatively early in the history of the GC in order to pollute the second generation of stars. In particular, we focus on NSMs that are induced from dynamical encounters, and those that are born and evolve as isolated binary pairs in the GC. Our main conclusions are

1. Dynamically-hardened DNSs merge far too late to contribute to *r*-process enrichment; even when the most liberal assumptions about NS segregation are assumed.
2. For the primordial binary population to contribute enough NSMs enrichment candidates, DNSs *must* be allowed to proceed through a phase of Case BB MT.
3. The stability of Case BB MT affects the number of enrichment candidates in GCs by about a factor of 2; if Case BB MT typically proceeds stably we find NSM enrichment events in  $\sim 2\text{--}12\%$  of GCs and if it typically proceeds unstably  $\sim 4\text{--}25\%$  of GCs. This is in slight tension with the observed number of enriched GCs in (Roederer 2011), which found in a sample of 11 GCs that  $\sim 50\%$  exhibited signs of star-to-star *r*-process dispersion. However, this sample is not large enough to make definitive statements about the exact enrichment fraction in old, metal-poor GCs, and variations in the assumed initial cluster properties, binary fraction, and enrichment radius can further act to reconcile these numbers.
4. Significant stripping of the secondary DNS progenitor is required for the system to remain bound to the GC, such that the envelope mass prior to the second SN is  $\lesssim 0.1 M_{\odot}$ . However, the hardest DNS progenitors, with pre-SN orbital separations of  $\lesssim 0.2 R_{\odot}$ , will typically be ejected from the GC regardless of the amount the secondary was stripped.
5. Since most enrichment candidates are efficiently ejected from the GC and quickly evacuate the cluster environment, for NSMs to be viable enrichment candidates there *must* be dense, star-forming gas in the GC at the formation time of DNSs,  $\sim 30\text{--}50$  Myr after the initial burst of star formation.

If mechanisms for quickly replenishing the young GC with star-forming gas cannot be established, another mechanism for *r*-process enhancement in GCs is likely at play. The predicted rate density of collapsars is in line with the stellar mass available to a young GC, though a more detailed investigation of this scenario's ability to produce the chemical abundances observed in *r*-process enriched, metal poor GCs would be necessary.

MZ would like to Jeff Andrews, Pablo Marchant, Mario Spera, Katie Breivik, and Chris Belczynski for useful discussions regarding binary evolution and DNS populations, Steinn Sigurdsson and Fred Rasio for insights into GC initial conditions and multiple populations, Enrico Ramirez-Ruiz for many helpful talks about  $r$ -process enrichment, Claire Ye for discussions on NS populations in GCs, Nick Stone for conversations about other potential  $r$ -process scenarios, Seth Jacobson for constructive interpretations of  $r$ -process dispersion, and Chris Pankow for general all-around helpfulness. MZ greatly appreciates financial support from the IDEAS Fellowship, a research traineeship program supported by the National Science Foundation under grant DGE-1450006. CPLB is supported by the CIERA Board of Visitors Research Professorship. VK is supported by a CIFAR G+EU Fellowship and Northwestern University. Research at

Perimeter Institute is supported in part by the Government of Canada through the Department of Innovation, Science and Economic Development Canada and by the Province of Ontario through the Ministry of Economic Development, Job Creation and Trade. The majority of our analysis was performed using the computational resources of the Quest high performance computing facility at Northwestern University, which is jointly supported by the Office of the Provost, the Office for Research, and Northwestern University Information Technology. This work was performed in part at Aspen Center for Physics, which is supported by National Science Foundation grant PHY-1607611.

*Software:* Astropy (The Astropy Collaboration et al. 2013, 2018), IPython (Pérez & Granger 2007), matplotlib (Hunter 2007), numpy (Oliphant 2006), pandas (McKinney 2010), scipy (Jones et al. 2001).

## REFERENCES

- Abbott, B. P., Abbott, R., Abbott, T. D., et al. 2017a, The Astrophysical Journal Letters, 848, L12.  
<http://iopscience.iop.org/article/10.3847/2041-8213/aa91c9>
- . 2017b, The Astrophysical Journal Letters, 850, L39.  
<http://arxiv.org/abs/1710.05836>  
<https://doi.org/10.3847/2041-8213/aa9478>
- . 2018, 1. <http://arxiv.org/abs/1811.12907>
- Alfaro, E. J., & Román-Zúñiga, C. G. 2018, Monthly Notices of the Royal Astronomical Society: Letters, 478, L110
- Amaro-Seoane, P., & Chen, X. 2016, Monthly Notices of the Royal Astronomical Society, 458, 3075
- Andrews, J. J., Farr, W. M., Kalogera, V., & Willems, B. 2015, Astrophysical Journal, 801, doi:10.1088/0004-637X/801/1/32
- Andrews, J. J., & Zezas, A. 2019, 16, 1.  
<http://arxiv.org/abs/1904.06137>
- Antognini, J. M., Shappee, B. J., Thompson, T. A., & Amaro-seoane, P. 2014, Monthly Notices of the Royal Astronomical Society, 439, 1079
- Arnould, M., Goriely, S., & Takahashi, K. 2007, Physics Reports, 450, 97
- Askar, A., Sedda, M. A., & Giersz, M. 2018, Monthly Notices of the Royal Astronomical Society, 478, 1844
- Askar, A., Szkudlarek, M., Gondek-Rosińska, D., Giersz, M., & Bulik, T. 2017, Monthly Notices of the Royal Astronomical Society, 464, 36. <http://arxiv.org/abs/1608.02520>  
<https://doi.org/10.1093/mnras/517/1>
- Banerjee, S. 2017, Monthly Notices of the Royal Astronomical Society, 467, 524
- Bastian, N., & Lardo, C. 2018, Annual Review of Astronomy and Astrophysics, 56, 83
- Bekki, K., & Tsujimoto, T. 2017, The Astrophysical Journal, 844, 34. <http://arxiv.org/abs/1706.01194>  
<https://doi.org/10.3847/1538-4357/aa77ae>
- Belczyński, K., Kalogera, V., & Bulik, T. 2002, The Astrophysical Journal, 527, 407. <http://arxiv.org/abs/astro-ph/0111452>
- Belczynski, K., Kalogera, V., Rasio, F. A., et al. 2008, The Astrophysical Journal Supplement Series, 174, 223.  
<http://arxiv.org/abs/astro-ph/0511811>  
<https://doi.org/10.1086/521026>
- Bellazzini, M., Fusi Pecci, F., Messineo, M., Monaco, L., & Rood, R. T. 2002, A, 123, 1509.  
<http://stacks.iop.org/1538-3881/123/i=3/a=1509>
- Beniamini, P., & Piran, T. 2016, Monthly Notices of the Royal Astronomical Society, 456, 4089
- Blaauw, A. 1961, Bulletin of the Astronomical Institutes of the Netherlands, XV
- Bonetti, M., Perego, A., Dotti, M., & Cescutti, G. 2019, 17, 1.  
<http://arxiv.org/abs/1905.12016>
- Boyles, J., Lorimer, D. R., Turk, P. J., et al. 2011, Astrophysical Journal, 742, doi:10.1088/0004-637X/742/1/51
- Bray, J. C., & Eldridge, J. J. 2018, Monthly Notices of the Royal Astronomical Society, 480, 5657
- Breivik, K., Coughlin, S., Zevin, M., et al. 2019, cosmic-popsynth, Zenedo, doi:http://doi.org/10.5281/zenodo.2642803
- Brisken, W. F., Benson, J. M., & Goss, W. M. 2002, The Astrophysical Journal, 571, 906
- Cescutti, G., Romano, D., Matteucci, F., Chiappini, C., & Hirschi, R. 2015, Astronomy & Astrophysics, 577, A139
- Chatterjee, S., Fregeau, J. M., Umbreit, S., & Rasio, F. A. 2010, Astrophysical Journal, 719, 915



- Chatterjee, S., Rasio, F. A., Sills, A., & Glebbeek, E. 2013, *Astrophysical Journal*, 777, doi:10.1088/0004-637X/777/2/106
- Chornock, R., Berger, E., Kasen, D., et al. 2017, *The Astrophysical Journal Letters*, 848, L19.  
<http://arxiv.org/abs/1710.05454>  
<https://doi.org/10.3847/2041-8213/aa905c>
- Chruslinska, M., Belczynski, K., Klencki, J., & Benacquista, M. 2018, *Monthly Notices of the Royal Astronomical Society*, 474, 2937
- Ciolfi, R., Kastaun, W., Giacomazzo, B., et al. 2017, *Physical Review D*, 95, 1
- Claeys, J. S. W., Pols, O. R., Izzard, R. G., Vink, J., & Verbunt, F. W. M. 2014, *Astronomy & Astrophysics*, 563, arXiv:1401.2895.  
<http://arxiv.org/abs/1401.2895>  
<https://doi.org/10.1051/0004-6361/201322714>
- Côté, B., Fryer, C. L., Belczynski, K., et al. 2017, *The Astrophysical Journal*, 855, 99.  
<http://arxiv.org/abs/1710.05875>  
<https://doi.org/10.3847/1538-4357/aaad67>
- Côté, B., Eichler, M., Arcones, A., et al. 2019, *The Astrophysical Journal*, 875, 106. <http://arxiv.org/abs/1809.03525>
- Cowan, J. J., Sneden, C., Lawler, J. E., et al. 2019, arXiv:1901.01410. <http://arxiv.org/abs/1901.01410>
- Cowperthwaite, P. S., Berger, E., Villar, V. A., et al. 2017, *The Astrophysical Journal Letters*, 848, 10.  
<http://arxiv.org/abs/1710.05840>  
<https://doi.org/10.3847/2041-8213/aa8fc7>
- Davies, M. B., Benz, W., Piran, T., & Thielemann, F. K. 1994, *The Astrophysical Journal*, 431, 742
- Delgado, A., & Thomas, H.-C. 1981, *Astronomy & Astrophysics*, 96, 142
- Dessart, L., Ott, C. D., Burrows, A., Rosswog, S., & Livne, E. 2009, *Astrophysical Journal*, 690, 1681
- Dewi, J. D., Pols, O. R., Savonije, G. J., & Van Den Heuvel, E. P. 2002, *Monthly Notices of the Royal Astronomical Society*, 331, 1027
- Dominik, M., Belczynski, K., Fryer, C., et al. 2012, *Astrophysical Journal*, 759, arXiv:1202.4901
- Eichler, D., Liviot, M., Piran, T., & Schramm, D. N. 1989, *Nature*, 340, 126
- Fernández, R., & Metzger, B. D. 2013, *Monthly Notices of the Royal Astronomical Society*, 435, 502
- Fragione, G., Grishin, E., Leigh, N. W. C., Perets, H. B., & Perna, R. 2018, 000, arXiv:1811.10627.  
<http://arxiv.org/abs/1811.10627>
- Fregeau, J. M., Cheung, P., Zwart, S. F. P., & Rasio, F. A. 2004, *Monthly Notices of the Royal Astronomical Society*, 352, 1
- Fregeau, J. M., Gurkan, M. A., Joshi, K. J., & Rasio, F. A. 2003, *The Astronomical Journal*, 593, 772.  
<http://arxiv.org/abs/astro-ph/0301521>  
<https://doi.org/10.1086/376593>
- Fregeau, J. M., & Rasio, F. A. 2007, *The Astrophysical Journal*, 658, 1047. [http://adsabs.harvard.edu/cgi-bin/nph-data?\\_query=bibcode=2007ApJ...658.1047F&link=\\_type=EJOURNAL](http://adsabs.harvard.edu/cgi-bin/nph-data?_query=bibcode=2007ApJ...658.1047F&link=_type=EJOURNAL)  
<https://arxiv.org/abs/0705201>
- Freiburghaus, C., Rosswog, S., & Thielemann, F.-K. 1999, *The Astrophysical Journal*, 525, L121.  
<http://stacks.iop.org/1538-4357/525/i=2/a=L121>
- Fryer, C., & Kalogera, V. 1997, *The Astrophysical Journal*, 489, 244
- Fryer, C. L., Belczynski, K., Wiktorowicz, G., et al. 2012, *The Astrophysical Journal*, 749, arXiv:1110.1726
- Giacobbo, N., Mapelli, M., & Spera, M. 2018, *Monthly Notices of the Royal Astronomical Society*, 474, 2959
- Giesler, M., Clausen, D., & Ott, C. D. 2018, *Monthly Notices of the Royal Astronomical Society*, 477, 1853
- Goldstein, A., Connaughton, V., Briggs, M. S., & Burns, E. 2015, *The Astrophysical Journal*, 818, 18.  
<http://arxiv.org/abs/1512.04464>  
<https://doi.org/10.3847/0004-637X/818/1/18>
- Gratton, R. G., Carretta, E., & Bragaglia, A. 2012, *Astronomy and Astrophysics Review*, 20, doi:10.1007/s00159-012-0050-3
- Grindlay, J., Zwart, S. F. P., & McMillan, S. 2006, *Nature Physics*, 214, doi:10.1038/nphys214
- Gurkan, M. A., Freitag, M., & Rasio, F. A. 2004, *The Astrophysical Journal*, 604, 632
- Halevi, G., & Mösta, P. 2018, *Monthly Notices of the Royal Astronomical Society*, 477, 2366
- Hansen, T. T., Holmbeck, E. M., Beers, T. C., et al. 2018, *The Astrophysical Journal*, 858, 92.  
<http://arxiv.org/abs/1809.09156>  
<https://doi.org/10.3847/1538-4357/aae9df>
- Hénon, M. 1971a, *Astrophysics and Space Science*, 13, 284
- . 1971b, *Astrophysics and Space Science*, 14, 151
- Herrera, C., & Boulanger, F. 2017, *Astronomy & Astrophysics*, 600, 1. <http://arxiv.org/abs/1701.00835>  
<https://doi.org/10.1051/0004-6361/201628454>
- Hobbs, G., Lorimer, D. R., Lyne, A. G., & Kramer, M. 2005, *Monthly Notices of the Royal Astronomical Society*, 360, 974
- Hong, J., Vesperini, E., Askar, A., et al. 2018, *Monthly Notices of the Royal Astronomical Society*, 480, 5645
- Hotokezaka, K., Beniamini, P., & Piran, T. 2018, *International Journal of Modern Physics D*, 27, arXiv:1801.01141.  
<http://arxiv.org/abs/1801.01141>  
<https://doi.org/10.1142/S0218271818420051>
- Hotokezaka, K., Kyutoku, K., Tanaka, M., et al. 2013, *Astrophysical Journal Letters*, 778, 1

- Hotokezaka, K., Piran, T., & Paul, M. 2015, *Nature Physics*, 11, 1042
- Hunter, J. D. 2007, *Computing in Science and Engineering*, 9, 99
- Hurley, J. R. 2007, *Monthly Notices of the Royal Astronomical Society*, 379, 93
- Hurley, J. R., Pols, O. R., & Tout, C. A. 2000, *Monthly Notices of the Royal Astronomical Society*, 315, 543
- Hurley, J. R., Tout, C. A., & Pols, O. R. 2002, *Monthly Notices of the Royal Astronomical Society*, 329, 897
- Ito, H., Aoki, W., Honda, S., & Beers, T. C. 2009, *Astrophysical Journal*, 698, 37
- Ivanova, N., Belczynski, K., Fregeau, J. M., & Rasio, F. A. 2005, *Monthly Notices of the Royal Astronomical Society*, 358, 572
- Ivanova, N., Belczynski, K., Kalogera, V., Rasio, F. A., & Taam, R. E. 2003, *The Astrophysical Journal*, 592, 475.  
<http://adsabs.harvard.edu/abs/2003ApJ...592..475I>
- Ivanova, N., Heinke, C. O., Rasio, F. A., Belczynski, K., & Fregeau, J. M. 2008, *Monthly Notices of the Royal Astronomical Society*, 386, 553
- Ivanova, N., & Taam, R. E. 2004, *The Astronomical Journal*, 601, 1058
- Ji, J., & Bregman, J. N. 2015, *Astrophysical Journal*, 807, 32.  
<http://dx.doi.org/10.1088/0004-637X/807/1/32>
- Jones, E., Oliphant, T. E., Peterson, P., & Others. 2001, *SciPy: Open source scientific tools for Python*, . . <http://www.scipy.org/>
- Joshi, K. J., Nave, C. P., & Rasio, F. A. 2001, *The Astrophysical Journal*, 550, 691.  
<http://stacks.iop.org/0004-637X/550/i=2/a=691>
- Joshi, K. J., Rasio, F. A., & Portegies Zwart, S. P. 2000, *ApJ*, 540, 969. <http://adsabs.harvard.edu/abs/2000ApJ...540..969J>
- Just, O., Bauswein, A., Ardevol Pulpillo, R., Goriely, S., & Janka, H. T. 2015, *Monthly Notices of the Royal Astronomical Society*, 448, 541
- Kajino, T., Aoki, W., Balantekin, A. B., et al. 2019, arXiv:1906.05002. <http://arxiv.org/abs/1906.05002>  
<http://dx.doi.org/10.1013/j.pnpnp.2019.02.008>
- Kalogera, V. 1996, *Astrophysical Journal*, 471, 352.  
<http://adsabs.harvard.edu/cgi-bin/nph-bib{ }query?bibcode=1996ApJ...471..352K{ }&db{ }key=AST>
- Kasen, D., Metzger, B., Barnes, J., Quataert, E., & Ramirez-Ruiz, E. 2017, *Nature*, 551, 80. <http://dx.doi.org/10.1038/nature24453>
- Kimmig, B., Seth, A., Ivans, I. I., et al. 2015, *Astronomical Journal*, 149, 53. <http://dx.doi.org/10.1088/0004-6256/149/2/53>
- Komiya, Y., & Shigeyama, T. 2016, *The Astrophysical Journal*, 830, 1. <http://dx.doi.org/10.3847/0004-637X/830/2/76http://arxiv.org/abs/1608.01772>  
<http://dx.doi.org/10.3847/0004-637X/830/2/76>
- Kremer, K., Lu, W., Rodriguez, C. L., Lachat, M., & Rasio, F. 2019a, arXiv:1904.06353. <http://arxiv.org/abs/1904.06353>
- Kremer, K., Ye, C. S., Chatterjee, S., Rodriguez, C. L., & Rasio, F. A. 2018, *The Astrophysical Journal Letters*, 855, L15.  
<http://arxiv.org/abs/1802.09553>  
<http://dx.doi.org/10.3847/2041-8213/aab26c>
- Kremer, K., Rodriguez, C. L., Amaro-Seoane, P., et al. 2019b, *Physical Review D*, 99, 63003.  
<https://doi.org/10.1103/PhysRevD.99.063003>
- Kroupa, P. 2001, *Monthly Notices of the Royal Astronomical Society*, 322, 231
- Kroupa, P., & Jerabkova, T. 2018, arXiv:1806.10605.  
<http://arxiv.org/abs/1806.10605>
- Kruckow, M. U., Tauris, T. M., Langer, N., et al. 2016, *Astronomy & Astrophysics*, 596, arXiv:1610.04417.  
<http://arxiv.org/abs/1610.04417>  
<http://dx.doi.org/10.1051/0004-6361/201629420>
- Kulkarni, S. R., Hut, P., & McMillan, S. J. 1993, *Nature*, 364, 421
- Lattimer, J. M., & Schramm, D. N. 1974, *The Astronomical Journal*, 192, L145
- . 1976, *The Astrophysical Journal*, 210, 549
- Lattimer, J. M., & Yahil, A. 1989, *The Astronomical Journal*, 340, 426
- Lee, W. H., Ramirez-Ruiz, E., & De Van Ven, G. 2010, *Astrophysical Journal*, 720, 953
- Leonard, P. J. T., Richer, H. B., & Fahlman, G. G. 1992, *The Astrophysical Journal*, 104, 2104
- Leroy, A. K., Bolatto, A. D., Ostriker, E. C., et al. 2018, *The Astrophysical Journal*, 869, 126.  
<http://arxiv.org/abs/1804.02083>  
<http://dx.doi.org/10.3847/1538-4357/aaecd1>
- Li, W., Chornock, R., Leaman, J., et al. 2011, *Monthly Notices of the Royal Astronomical Society*, 412, 1473
- Liang, E., Zhang, B., Virgili, F., & Dai, Z. G. 2007, *The Astrophysical Journal*, 662, 1111
- Lovegrove, E., & Woosley, S. E. 2013, *Astrophysical Journal*, 769, 2
- Lucatello, S., Sollima, A., Gratton, R., et al. 2015, *Astronomy & Astrophysics*, 584, A52
- MacFadyen, A. I., & Woosley, S. E. 1999, *The Astrophysical Journal*, 524, 262
- Macias, P., & Ramirez-Ruiz, E. 2019, arXiv:1905.04315.  
<http://arxiv.org/abs/1905.04315>
- Mackey, A. D., Wilkinson, M. I., Davies, M. B., & Gilmore, G. F. 2007, *Monthly Notices of the Royal Astronomical Society: Letters*, 379, 40
- . 2008, *Monthly Notices of the Royal Astronomical Society: Letters*, 386, 65
- Madau, P. 2017, *The Astrophysical Journal*, 851, 50.  
<http://arxiv.org/abs/1710.07636>  
<http://dx.doi.org/10.3847/1538-4357/aa9715>

- Marks, M., Kroupa, P., Dabringhausen, J., & Pawlowski, M. S. 2012, *Monthly Notices of the Royal Astronomical Society*, 422, 2246
- Martínez-Pinedo, G., Fischer, T., Lohs, A., & Huther, L. 2012, *Physical Review Letters*, 109, 1
- McKinney, W. 2010, *Proceedings of the 9th Python in Science Conference*. <http://pandas.sourceforge.net>
- Metzger, B. D., Thompson, T. A., & Quataert, E. 2008, *The Astrophysical Journal*, 676, 1130
- Meyer, B. S. 1989, *The Astrophysical Journal*, 343, 254
- Meylan, G., & Heggie, D. C. 1997, *Astronomy and Astrophysics Review*, 8, 1
- Miyaji, S., Nomoto, K., Yokoi, K., & Sugimoto, D. 1980, *Publications of the Astronomical Society of Japan*, 32, 303
- Morscher, M., Pattabiraman, B., Rodriguez, C., Rasio, F. A., & Umbreit, S. 2015, *Astrophysical Journal Letters*, 800, doi:10.1088/0004-637X/800/1/9
- Mösta, P., Roberts, L. F., Halevi, G., et al. 2018, *The Astrophysical Journal*, 864, 171. <http://dx.doi.org/10.3847/1538-4357/aad6e><http://arxiv.org/abs/1712.09370>
- Mösta, P., Richers, S., Ott, C. D., et al. 2014, *Astrophysical Journal Letters*, 785, 1
- Nomoto, K. 1984, *The Astrophysical Journal*, 277, 791
- . 1987, *The Astrophysical Journal*, 322, 206
- Oechlin, R., Janka, H.-T., & Marek, A. 2007, *Astronomy & Astrophysics*, 467, 395
- Oliphant, T. E. 2006, *A guide to NumPy* (Trelgol Publishing USA)
- Parker, R. J. 2018, *Monthly Notices of the Royal Astronomical Society*, 476, 617
- Pattabiraman, B., Umbreit, S., Liao, W. K., et al. 2013, *Astrophysical Journal, Supplement Series*, 204, doi:10.1088/0067-0049/204/2/15
- Pérez, F., & Granger, B. E. 2007, *IEEE Journals & Magazines*, 9, 21
- Perley, D. A., Krühler, T., Schulze, S., et al. 2016, *The Astrophysical Journal*, 817, 7
- Peters, P. C. 1964, *Physical Review*, 136, 1224
- Pfahl, E., Rappaport, S., & Podsiadlowski, P. 2002, *The Astrophysical Journal*, 573, 283
- Placco, V. M., Frebel, A., Lee, Y. S., et al. 2015, *Astrophysical Journal*, 809, 136. <http://dx.doi.org/10.1088/0004-637X/809/2/136>
- Plummer, H. C. 1911, *Monthly Notices of the Royal Astronomical Society*, 71, 460
- Podsiadlowski, P., Langer, N., Poelarends, a. J. T., et al. 2004, *The Astrophysical Journal*, 612, 1044. <http://arxiv.org/abs/astro-ph/0309588>
- Qian, Y. Z., & Woosley, S. E. 1996, *The Astrophysical Journal*, 471, 331. <http://arxiv.org/abs/astro-ph/9611094><http://dx.doi.org/10.1086/177973>
- Ramirez-Ruiz, E., Trenti, M., MacLeod, M., et al. 2015, *Astrophysical Journal Letters*, 802, L22. <http://dx.doi.org/10.1088/2041-8205/802/2/L22>
- Raskutti, S., Ostriker, E. C., & Skinner, M. A. 2016, *The Astrophysical Journal*, 829, 1. <http://arxiv.org/abs/1608.04469><http://dx.doi.org/10.3847/0004-637X/829/2/130>
- Roberts, L. F., Reddy, S., & Shen, G. 2012, *Physical Review C - Nuclear Physics*, 86, 1
- Rodriguez, C. L., Amaro-seoane, P., Chatterjee, S., et al. 2018a, *Physical Review D*, 98, 123005. <https://doi.org/10.1103/PhysRevD.98.123005>
- Rodriguez, C. L., Amaro-Seoane, P., Chatterjee, S., et al. 2018b, *Physical Review D*, in press, arXiv:1811.04926
- Rodriguez, C. L., Chatterjee, S., & Rasio, F. A. 2016, *Physical Review D*, 93, 1
- Rodriguez, C. L., Morscher, M., Pattabiraman, B., et al. 2015, *Physical Review Letters*, 115, 1
- Roederer, I. U. 2011, *Astrophysical Journal Letters*, 732, 1
- Roederer, I. U., & Sneden, C. 2011, *Astronomical Journal*, 142, arXiv:1104.5055
- Rosswog, S., & Liebend, M. 1999, *Astronomy & Astrophysics*, 341, 499
- Rubenstein, E. P., & Bailyn, C. D. 1997, *The Astrophysical Journal*, 474, 701
- Ruffert, M., Janka, H. T., Takahashi, K., & Schaefer, G. 1997, *Astronomy & Astrophysics*, 319, 122. <http://arxiv.org/abs/astro-ph/9606181>
- Safarzadeh, M., Ramirez-Ruiz, E., Andrews, J. J., et al. 2018, *The Astrophysical Journal*, 872, 105. <http://arxiv.org/abs/1810.04176>
- Sakari, C. M., Placco, V. M., Farrell, E. M., et al. 2018, *The Astrophysical Journal*, 868, 110. <http://arxiv.org/abs/1809.09156><http://dx.doi.org/10.3847/1538-4357/aae9df>
- Samsing, J., MacLeod, M., & Ramirez-Ruiz, E. 2014, *The Astrophysical Journal*, 784, 71. <http://stacks.iop.org/0004-637X/784/i=1/a=71?key=crossref.745c323f94ee6338fdd625bc13a2699e>
- Sana, H., James, G., & Gosset, E. 2011, *Monthly Notices of the Royal Astronomical Society*, 416, 817
- Schwab, J., Podsiadlowski, P., & Rappaport, S. 2010, *Astrophysical Journal*, 719, 722
- Shen, S., Cooke, R. J., Ramirez-Ruiz, E., et al. 2015, *Astrophysical Journal*, 807, 115. <http://dx.doi.org/10.1088/0004-637X/807/2/115>

- Siegel, D. M. 2019, 170817, arXiv:1901.09044.  
<http://arxiv.org/abs/1901.09044>
- Siegel, D. M., Barnes, J., & Metzger, B. D. 2019, *Nature*, 569, 241.  
<http://dx.doi.org/10.1038/s41586-019-1136-0>
- Siegel, D. M., Ciolfi, R., & Rezzolla, L. 2014, *Astrophysical Journal Letters*, 785, doi:10.1088/2041-8205/785/1/L6
- Siegel, D. M., & Metzger, B. D. 2017, *Physical Review Letters*, 119, 1
- Sigurdsson, S., & Phinney, E. S. 1993, *The Astrophysical Journal*, 39, 631
- Skinner, M. A., & Ostriker, E. C. 2015, *Astrophysical Journal*, 809, 187. <http://dx.doi.org/10.1088/0004-637X/809/2/187>
- Snedden, C., Shetrone, M. D., Kraft, R. P., et al. 1997, *The Astronomical Journal*, 114, 1964
- Sobeck, J. S., Kraft, R. P., Sneden, C., et al. 2011, *Astronomical Journal*, 141, doi:10.1088/0004-6256/141/6/175
- Spitzer, L. 1987, *Dynamical evolution of globular clusters* (Princeton, N.J.: Princeton University Press, c1987)
- Stanek, K., Gnedin, O., Beacom, J., et al. 2006, *ACTA Astronomica*, 56, 333
- Tanvir, N. R., Levan, A. J., Gonzalez-Fernandez, C., et al. 2017, *The Astrophysical Journal Letters*, 848, L27.  
<http://arxiv.org/abs/1710.05455>  
<http://dx.doi.org/10.3847/2041-8213/aa90b6>
- Tauris, T. M., Langer, N., Moriya, T. J., et al. 2013, *Astrophysical Journal Letters*, 778, 2
- Tauris, T. M., Langer, N., & Podsiadlowski, P. 2015, *Monthly Notices of the Royal Astronomical Society*, 451, 2123
- Tauris, T. M., & Takens, R. J. 1998, *Astron. Astrophys.*, 330, 1047.  
<https://pdfs.semanticscholar.org/a400/e4ac71be41402142830fc8e62bd1d0a009ec.pdf>
- Tauris, T. M., Kramer, M., Freire, P. C. C., et al. 2017, *The Astrophysical Journal*, 846, 170.  
<http://arxiv.org/abs/1706.09438>  
<http://dx.doi.org/10.3847/1538-4357/aa7e89>
- The Astropy Collaboration, Robitaille, T. P., Tollerud, E. J., et al. 2013, *Astronomy & Astrophysics*, 558, A33.  
<http://arxiv.org/abs/1307.6212>  
<http://dx.doi.org/10.1051/0004-6361/201322068>
- The Astropy Collaboration, Price-Whelan, A. M., Sipőscz, B. M., et al. 2018, *The Astronomical Journal*, 156, 123.  
<http://arxiv.org/abs/1801.02634>  
<http://dx.doi.org/10.3847/1538-3881/aabc4f>
- Thompson, T. A., Burrows, A., & Meyer, B. M. 2001, *The Astrophysical Journal*, 562, 887
- Thompson, T. A., Chang, P., & Quataert, E. 2004, *The Astrophysical Journal*, 611, 380
- Tsang, B. T., & Milosavljević, M. 2018, *Monthly Notices of the Royal Astronomical Society*, 478, 4142
- van de Voort, F., Quataert, E., Hopkins, P. F., Kereš, D., & Faucher-Giguère, C. A. 2015, *Monthly Notices of the Royal Astronomical Society*, 447, 140
- Vanzella, E., Calura, F., Meneghetti, M., et al. 2017, *Monthly Notices of the Royal Astronomical Society*, 467, 4304
- . 2018, *Monthly Notices of the Royal Astronomical Society*, 483, 3618. <http://arxiv.org/abs/1809.02617>
- Vigna-Gómez, A., Neijssel, C. J., Stevenson, S., et al. 2018, *Monthly Notices of the Royal Astronomical Society*, 481, 4009
- Villar, V. A., Guillochon, J., Berger, E., et al. 2017, *The Astrophysical Journal Letters*, 851, L21.  
<http://arxiv.org/abs/1710.11576>  
<http://dx.doi.org/10.3847/2041-8213/aa9c84>
- Vink, J. S., & de Koter, A. 2005, *Astronomy & Astrophysics*, 442, 587
- Vink, J. S., de Koter, A., & Lamers, H. J. G. L. M. 2001, *Astronomy & Astrophysics*, 369, 574.  
<http://dx.doi.org/10.1051/0004-6361:20041017>
- Wallner, A., Faermann, T., Feige, J., et al. 2015, *Nature Communications*, 6, 1. <http://dx.doi.org/10.1038/ncomms6956>
- Wanderman, D., & Piran, T. 2010, *Monthly Notices of the Royal Astronomical Society*, 406, 1944
- Webb, J. J., & Leigh, N. W. 2015, *Monthly Notices of the Royal Astronomical Society*, 453, 3278
- Webbink, R. 1984, *Astrophysical Journal*, 277, 355
- Wehmeyer, B., Pignatari, M., & Thielemann, F. K. 2015, *Monthly Notices of the Royal Astronomical Society*, 452, 1970
- Wex, N., Kalogera, V., & Kramer, M. 2002, *The Astrophysical Journal*, 528, 401
- Winteler, C., Käppeli, R., Perego, A., et al. 2012, *Astrophysical Journal Letters*, 750, doi:10.1088/2041-8205/750/1/L22
- Wong, T.-W., Willems, B., & Kalogera, V. 2010, *The Astrophysical Journal*, 721, 1689. [http://adsabs.harvard.edu/cgi-bin/nph-data?\\_query=bibcode=2010ApJ...721.1689W&link\\_type=ABSTRACT](http://adsabs.harvard.edu/cgi-bin/nph-data?_query=bibcode=2010ApJ...721.1689W&link_type=ABSTRACT)  
<http://publication/doi/10.1088/0004-637X/721/2/1689>
- Woosley, S. E. 1993, *The Astronomical Journal*, 405, 273
- . 2016, *The Astrophysical Journal*, 836, 1.  
<http://arxiv.org/abs/1608.08939>  
<http://dx.doi.org/10.3847/1538-4357/836/2/244>
- Worley, C. C., Hill, V., Sobeck, J., & Carretta, E. 2013, *Astronomy & Astrophysics*, 553, A47
- Ye, C. S., Kremer, K., Chatterjee, S., Rodriguez, C. L., & Rasio, F. A. 2019, arXiv:1902.05963. <http://arxiv.org/abs/1902.05963>
- Yong, D., Aoki, W., Lambert, D. L., & Paulson, D. B. 2006, *The Astrophysical Journal*, 639, 918
- Yong, D., & Grundahl, F. 2008, *The Astrophysical Journal*, 672, L29



Zevin, M., Samsing, J., Rodriguez, C., Haster, C.-J., &  
Ramirez-Ruiz, E. 2018, The Astrophysical Journal, 871, 91.  
<http://arxiv.org/abs/1810.00901>

Zwart, S. P., McMillan, S., & Gieles, M. 2010, Annual Review of  
Astronomy and Astrophysics, 48, 431.  
<http://arxiv.org/abs/1002.1961>{%}0Ahttp:  
[//dx.doi.org/10.1146/annurev-astro-081309-130834](https://doi.org/10.1146/annurev-astro-081309-130834)

## APPENDIX

## A. TREATMENT OF SN KICKS FOLLOWING A CE PHASE

One notable change in Models B–E compared to Model A is how SN kicks are implemented during CE evolution. By default, BSE treats this in a self-inconsistent way that leads to artificially inflated post-SN systemic velocities. The final separation of the donor star’s core and the compact companion is calculated using standard energetics arguments as in [Webbink \(1984\)](#). The orbital hardening during a CE phase is calculated by the energy necessary to eject the envelope:

$$E_{\text{bind, i}} = \alpha_{\text{CE}}(E_{\text{orb, f}} - E_{\text{orb, i}}), \quad (\text{A1})$$

$$-\frac{G}{\lambda} \left( \frac{M(M_{\star} - M_{\star, \text{c}})}{R_{\star}} \right) = -\alpha_{\text{CE}} \frac{GM_{\star, \text{c}}m_{\text{NS}}}{2} \left( \frac{1}{a_{\text{f}}} - \frac{1}{a_{\text{i}}} \right). \quad (\text{A2})$$

This can be solved for the final orbital separation as

$$a_{\text{f}} = \frac{\alpha_{\text{CE}} \lambda R_{\star} M_{\star, \text{c}} m_{\text{NS}} a_{\text{i}}}{2M_{\star} a_{\text{i}} (M_{\star} - M_{\star, \text{c}}) + \alpha_{\text{CE}} \lambda R_{\star} M_{\star, \text{c}} m_{\text{NS}}}, \quad (\text{A3})$$

where  $\alpha_{\text{CE}}$  is the CE efficiency parameter,  $\lambda$  is the envelope binding energy parameter which adjusts the amount of energy needed from the orbit to eject the envelope, and  $M_{\star}$ ,  $M_{\star, \text{c}}$ , and  $R_{\star}$  are the donor star’s total mass, core mass, and radius, respectively.

If a star evolves into a NS or BH immediately after the CE, the function for implementing the SN kick is called. However, in default BSE, at this point the pre-SN mass of the exploding star is reset to its value prior to the CE (i.e. it does not account for the envelope mass that is ejected during the CE spiral-in to bring the pre-SN binary to its tightened orbital configuration), leading to a large amount of mass-loss during the SN at a tight pre-SN orbital separation. This issue is especially drastic when dealing with CEs involving an evolved naked He star, as the cores of the stars can reach extremely hardened separations of  $\approx 0.1 R_{\odot}$ . The contribution of the mass-loss Blaauw kick on the post-SN systemic velocity is

$$v_{\text{sys, Blaauw}} \approx 220 \left( \frac{\Delta M_{\text{SN}}}{M_{\odot}} \right) \left( \frac{a_{\text{pre}}}{R_{\odot}} \right)^{-1/2} \left[ 2.8 + \left( \frac{\Delta M_{\text{SN}}}{M_{\odot}} \right) \right]^{-1/2} \text{ km s}^{-1}, \quad (\text{A4})$$

where  $\Delta M_{\text{SN}}$  is the mass lost in the SN,  $a_{\text{pre}}$  is the pre-SN orbital separation, and neutron-star masses are assumed to be  $1.4 M_{\odot}$ . The increased mass loss therefore leads to systematically higher post-SN systemic velocities. For example, a DNS progenitor at an orbital separation of  $0.1 R_{\odot}$  that loses  $1.5 M_{\odot}$  in the SN will achieve a post-SN systemic velocity solely from the Blaauw kick of  $\approx 500 \text{ km s}^{-1}$ . Therefore, even without natal kicks, newly born DNSs can be boosted to post-SN systemic velocities of  $\gtrsim 1000 \text{ km s}^{-1}$  solely due to mass loss in the SN. This inconsistency can strongly affect DNS systemic velocities, post-SN orbital properties, SN survival, and possibly merger rates from populations that are modeled using a modified BSE framework.